

Significance testing for canonical correlation analysis in high dimensions

Ian W. McKeague[†] and Xin Zhang[‡]

[†]*Columbia University* and [‡]*Florida State University*

Abstract

We consider the problem of testing for the presence of linear relationships between large sets of random variables based on a post-selection inference approach to canonical correlation analysis. The challenge is to adjust for the selection of subsets of variables having linear combinations with maximal sample correlation. To this end, we construct a stabilized one-step estimator of the euclidean-norm of the canonical correlations maximized over subsets of variables of pre-specified cardinality. This estimator is shown to be consistent for its target parameter and asymptotically normal provided the dimensions of the variables do not grow too quickly with sample size. We also develop a greedy search algorithm to accurately compute the estimator, leading to a computationally tractable omnibus test for the global null hypothesis that there are no linear relationships between any subsets of variables having the pre-specified cardinality. Further, we develop a confidence interval for the target parameter that takes the variable selection into account.

Key words: Efficient one-step estimator; Greedy search algorithm; Large-scale testing; Pillai trace; Post-selection inference

1 Introduction

When exploring the relationships between two sets of variables measured on the same set of observations, canonical correlation analysis (CCA; Hotelling, 1936) sequentially extracts linear combinations with maximal sample correlation. Specifically, with $\mathbf{X} \in \mathbb{R}^p$ and $\mathbf{Y} \in \mathbb{R}^q$ as two random vectors, the first step of CCA targets the parameter

$$\rho = \max_{\alpha \in \mathbb{R}^q, \beta \in \mathbb{R}^p} \text{corr}(\alpha^T \mathbf{Y}, \beta^T \mathbf{X}), \quad \text{subject to } \text{var}(\alpha^T \mathbf{Y}) = 1 = \text{var}(\beta^T \mathbf{X}). \quad (1)$$

Subsequent steps of CCA repeat this process subject to the constraint that the next linear combinations of \mathbf{X} (and \mathbf{Y}) are uncorrelated with earlier ones, giving a decreasing sequence of correlation coefficients. We are interested in testing whether the maximal canonical correlation coefficient

$\rho \neq 0$ versus the null hypothesis $\rho = 0$ in the high-dimensional setting in which p and q grow with sample size n . This is equivalent to testing whether all of the canonical correlation coefficients vanish, or whether their sum of squares τ^2 (known as the Pillai (1955) trace) vanishes.

Over the last dozen years, numerous sparse canonical correlation analysis (SCCA) methods (e.g., Witten et al., 2009; Haroon and Shawe-Taylor, 2011; Gao et al., 2017; Mai and Zhang, 2019; Qadar and Seghouane, 2019; Shu et al., 2020) have been developed as extensions of classical CCA by adapting regularization approaches from regression, e.g., lasso (Tibshirani, 1996), elastic net (Zou and Hastie, 2005) and soft thresholding.

SCCA methods have been widely applied to high-dimensional omics data to detect associations between gene expression and DNA copy number/polymorphisms/methylation, with the aim of revealing networks of co-expressed and co-regulated genes (Waaijenborg and Zwinderman, 2007; Waaijenborg et al., 2008; Naylor et al., 2010; Parkhomenko et al., 2009; Wang et al., 2015). A problem with the indiscriminate use of such methods, however, is *selection bias*, arising when the effects of variable selection on subsequent statistical analyses are ignored, i.e., failure to take into account “double dipping” of the data when assessing evidence of association.

Devising valid tests for associations in high-dimensional SCCA, along with confidence interval estimation for the strength of the association, poses a challenging post-selection inference problem. Nevertheless, some progress on this problem has been made. Yang and Pan (2015) proposed the sum of sample canonical correlation coefficients as a test statistic and established a valid calibration under the sparsity assumption that the number of non-zero canonical correlations is finite and fixed, with the dimensions p and q proportional to sample size. Their approach comes at the cost of assuming that \mathbf{X} and \mathbf{Y} are jointly Gaussian (and thus fully independent under the null); similar results for the maximal sample canonical correlation coefficient are developed in Bao et al. (2019). Zheng et al. (2019) developed a test for the presence of correlations among arbitrary components of a given high-dimensional random vector, for both sparse and dense alternatives, but their approach also requires an independent components structure.

In this paper, we provide valid post-selection inference for a new version of SCCA in high-dimensional settings. We obtain a computationally tractable and asymptotically valid confidence interval for τ_{\max} , where τ_{\max}^2 is the maximum of the Pillai trace over all subvectors of \mathbf{X} and \mathbf{Y} having prespecified dimensions s_x and s_y , respectively. The method is fully nonparametric

in the sense that no distributional assumptions or sparsity assumptions are required. Rather than adopting a penalization approach or making a sparsity assumption on the number of non-zero canonical correlations to regularize the problem, we use the sparsity levels $s_x \ll p$ and $s_y \ll q$ for regularization, and also for controlling the computational cost of searching over large collections of subvectors. We introduce a test statistic $\hat{\tau}_{\max}$ constructed as a stabilized and efficient one-step estimator of τ_{\max} . Then, assuming p and q do not grow too quickly with sample size, specifically that $\log(p + q)/\sqrt{n} \rightarrow 0$, we show that a studentized version of $\hat{\tau}_{\max}$ (after centering by τ_{\max}) converges weakly to standard normal. This leads to a practical way of calibrating a formal omnibus test for the global null hypothesis ($\tau_{\max} = 0$) that there are no linear relationships between any subsets of variables having the pre-specified cardinality, along with an asymptotically valid Wald-type confidence interval for τ_{\max} .

The proposed approach applies to any choice of pre-specified sparsity levels s_x and s_y , which do not need to be the same as the true number of “active” variables in the population CCA, although they should be sufficiently large to capture the key associations. The test procedure and confidence interval for the target parameter τ_{\max} are asymptotically valid for any pre-specified sparsity levels, and work well provided the sample cross-covariance matrices between subvectors of \mathbf{X} and \mathbf{Y} having dimensions s_x and s_y are sufficiently accurate.

Our approach is related to the type of post-selection inference procedure for marginal screening developed by McKeague and Qian (2015), which applies to the one-dimensional response case ($q = 1$ in the present notation). To extend this approach to the SCCA setting, in which both p and q can be large, requires a trade-off between computational tractability and statistical power. The calibration used in McKeague and Qian (2015) is a double-bootstrap technique, which is computationally expensive. To obtain a fast calibration method for SCCA, we adapt the sample-splitting stabilization technique of Luedtke and van der Laan (2018) to the SCCA setting, which provides calibration using a standard normal limit. Further, to control the computational complexity of searching through large collections of subvectors of \mathbf{X} and \mathbf{Y} when computing $\hat{\tau}_{\max}$, we develop a greedy search algorithm related to that of Wiesel et al. (2008).

The rest of the article is organized as follows. Section 2 introduces the population target parameter τ_{\max} and develops its stabilized one-step estimator, taking the non-regularity of τ_{\max} at the global null hypothesis into account; asymptotic results are given in Section 2.4. Section 3 pro-

poses the greedy search algorithm to speed up the computation and provides a rationale based on submodularity. Sections 4 and 5 respectively contain a simulation study and a real data example using data collected under the Cancer Genome Atlas Program (Weinstein et al., 2013). Section 6 concludes the paper with a short discussion. The Appendix contains a derivation of the influence function of the Pillai trace, which plays a key role in its efficient estimation, and the proof of an identity involving increments of the Pillai trace used in the greedy search algorithm. The Supplementary Materials collect all additional technical details, numerical results and R code.

2 Test procedure

2.1 Preliminaries

Let $\Sigma_{\mathbf{X}} > 0$ and $\Sigma_{\mathbf{Y}} > 0$ denote the (invertible) covariance matrices of \mathbf{X} and \mathbf{Y} , with cross-covariance matrix $\Sigma_{\mathbf{XY}}$ and standardized cross-covariance matrix $\Lambda_{\mathbf{XY}} \equiv \Sigma_{\mathbf{X}}^{-1/2} \Sigma_{\mathbf{XY}} \Sigma_{\mathbf{Y}}^{-1/2} \in \mathbb{R}^{p \times q}$ (also known as the coherence matrix). The sample counterparts are denoted $\mathbf{S}_{\mathbf{X}}$, $\mathbf{S}_{\mathbf{Y}}$, $\mathbf{S}_{\mathbf{XY}}$ and $\mathbf{C}_{\mathbf{XY}}$, respectively.

The coherence matrix $\Lambda_{\mathbf{XY}}$ has $\min(p, q)$ singular values; when listed in decreasing order they coincide with the canonical correlation coefficients, and ρ defined in (1) is the largest. A closely related parameter in MANOVA is the Pillai trace τ^2 (Pillai, 1955), defined as the sum of squares of the canonical correlation coefficients, or equivalently

$$\tau^2 = \|\Lambda_{\mathbf{XY}}\|_F^2 = \text{tr}(\Lambda_{\mathbf{XY}} \Lambda_{\mathbf{XY}}^T) = \text{tr}\{\mathbf{H}(\mathbf{H} + \mathbf{E})^{-1}\}, \quad (2)$$

where $\|\cdot\|_F$ is Frobenius norm, and $\mathbf{H} = \Sigma_{\mathbf{YX}} \Sigma_{\mathbf{X}}^{-1} \Sigma_{\mathbf{XY}}$ and $\mathbf{E} = \Sigma_{\mathbf{Y}} - \mathbf{H}$ are population versions of covariance matrices in a linear model for predicting \mathbf{Y} from \mathbf{X} . Specifically, \mathbf{H} is the covariance matrix of the least-squares-predicted outcome in the linear model $\mathbf{Y} = \mathbf{A} + \mathbf{B}\mathbf{X} + \boldsymbol{\varepsilon}$, where $\text{cov}(\boldsymbol{\varepsilon}) = \mathbf{E}$ and $\boldsymbol{\varepsilon}$ is uncorrelated with \mathbf{X} .

We will need some general concepts from semi-parametric efficiency theory. Suppose we observe a general random vector $\mathbf{O} \sim P$. Let $L_0^2(P)$ denote the Hilbert space of P -square integrable functions with mean zero. Consider a smooth one-dimensional family of probability measures $\{P_t, t \in [0, 1]\}$ with $P_0 = P$ and having score function $k \in L_0^2(P)$ at $t = 0$. The tangent space $T(P)$ is the $L_0^2(P)$ -closure of the linear span of all such score functions k . For example, if nothing is known about P , then $P_t(d\mathbf{o}) = (1 + tk(\mathbf{o}))P(d\mathbf{o})$ is such a submodel for any bounded

function k with mean zero (provided t is sufficiently small), so $T(P)$ is seen to be the whole of $L_0^2(P)$ in this case. Let $\psi(P)$ be a real parameter that is pathwise differentiable at P : there exists $g \in L_0^2(P)$ such that $\lim_{t \rightarrow 0} (\psi(P_t) - \psi(P)) / t = \langle g, k \rangle$, for any smooth submodel $\{P_t\}$ with score function k , where $\langle \cdot, \cdot \rangle$ is the inner product in $L_0^2(P)$. The function g is called a gradient (or influence function) for ψ ; the projection IF_ψ of any gradient into the tangent space $T(P)$ is unique and is known as the canonical gradient (or efficient influence function). The supremum of the Cramér–Rao bounds for all submodels (the information bound) is given by the second moment of $\text{IF}_\psi(\mathbf{O})$. Furthermore, the influence function as derived using von Mises calculus (van der Vaart, 2000, Chapter 20) of any regular and asymptotically linear estimator must be a gradient (Pfanzagl, 1990, Proposition 2.3).

A one-step estimator is an empirical bias correction of a naïve plug-in estimator in the direction of a gradient of the parameter of interest (Pfanzagl, 1982); when this gradient is the canonical gradient, then this results in an efficient estimator under some regularity conditions. Given an initial estimator \hat{P} of P and any gradient $D(\hat{P})$ of the parameter ψ evaluated at \hat{P} , we have $\psi(\hat{P}) - \psi(P) = -PD(\hat{P}) + \text{Rem}_\psi(\hat{P}, P)$, where $\text{Rem}_\psi(\hat{P}, P)$ is negligible if \hat{P} is close to P in an appropriate sense. Here Pf denotes the expectation under P of a random real-valued function f , ignoring the randomness in f . As $D(P)$ has mean zero under P , we expect that $PD(\hat{P})$ is close to zero if D is continuous in its argument and \hat{P} is close to P . However, the rate of convergence of $PD(\hat{P})$ to zero as sample size grows may be slower than $n^{-1/2}$. The one-step estimator aims to improve $\psi(\hat{P})$ and achieve $n^{1/2}$ -consistency and asymptotically normality by adding an empirical estimate $\mathbb{P}_n D(\hat{P})$ of its deviation from $\psi(P)$. The one-step estimator $\hat{\psi} \equiv \psi(\hat{P}) + \mathbb{P}_n D(\hat{P})$ then satisfies the expansion $\hat{\psi} - \psi(P) = (\mathbb{P}_n - P)D(\hat{P}) + \text{Rem}_\psi(\hat{P}, P)$. Under an empirical process and $L^2(P)$ consistency condition on $D(\hat{P})$, the leading term on the right is asymptotically equivalent to $(\mathbb{P}_n - P)D(P)$, which converges in distribution to a mean-zero Gaussian limit with consistently estimable covariance. To minimize the variance of the Gaussian limit, $D(\hat{P})$ can be taken as the canonical gradient of ψ at \hat{P} .

2.2 Maximal Pillai trace

Clearly, the null hypotheses $\rho = 0$ and $\tau = 0$ are equivalent, but the root-Pillai trace τ (the positive square root of the Pillai trace) is a more informative target parameter than the leading

canonical correlation ρ , although the two would coincide if there is only a single non-zero canonical correlation coefficient. Moreover, because estimating the maximal values of τ or ρ , subject to sparsity constraints, needs repeated evaluation and updating of the estimates, the choice of τ provides considerable computational savings over ρ , as the latter would require updating the entire eigen-decomposition at each step.

Our approach is to develop asymptotic distribution results for a regularized empirical version of this target parameter when the dimensions p and q grow with sample size n . Specifically, given sparsity levels s_x and s_y for \mathbf{X} and \mathbf{Y} , respectively, we are interested in selecting index sets $\mathcal{K} \subset \{1, \dots, p\}$ and $\mathcal{J} \subset \{1, \dots, q\}$ with cardinality $|\mathcal{K}| \leq s_x$ and $|\mathcal{J}| \leq s_y$ that maximize the Pillai trace (or equivalently the root-Pillai trace) of their corresponding sub-vectors. The sparsity levels s_x and s_y are pre-specified and fixed, e.g., $(s_x, s_y) = (1, 2)$.

Given independent observations $\mathbf{O}_i = (\mathbf{X}_i^T, \mathbf{Y}_i^T)^T$, $i = 1, \dots, n$, drawn from a distribution P on \mathbb{R}^{p+q} , we target the non-regular parameter

$$\tau_{\max} \equiv \max_{d \in \mathcal{D}_n} \Psi^d(P), \quad (3)$$

where $\mathcal{D}_n = \{(\mathcal{J}, \mathcal{K}) \mid |\mathcal{K}| = s_x \leq p, |\mathcal{J}| = s_y \leq q, \mathcal{K} \subseteq \{1, \dots, p\}, \mathcal{J} \subseteq \{1, \dots, q\}\}$ and $\Psi^d(P) = \|\Lambda_{\mathbf{X}_{\mathcal{K}}\mathbf{Y}_{\mathcal{J}}}\|_F$. Note that $\tau_{\max} \leq \tau$ with equality when $s_x = p$, $s_y = q$. The subscript n in \mathcal{D}_n indicates that the dimensions $p = p_n$ and $q = q_n$ are allowed to increase with n .

The numbers of active variables (s_x^*, s_y^*) are the smallest values of the sparsity levels (s_x, s_y) for which $\tau_{\max} = \tau$. Note that s_x^* and s_y^* can be as large as p and q , respectively, and as small as the number of non-zero canonical correlation coefficients for \mathbf{X} and \mathbf{Y} (the rank of $\Lambda_{\mathbf{X}\mathbf{Y}}$, denoted K in the sequel). The non-regularity arises for various reasons, including the fact that multiple elements of \mathcal{D}_n may achieve the same maximum in (3) (e.g., when $\tau_{\max} = 0$). This may occur, for example, if the pre-specified sparsity levels are larger than the true sparsity levels (s_x^*, s_y^*) , but as we see later in this section the sample root-Pillai trace is non-regular at $\tau_{\max} = 0$ even when d is fixed.

We now use von Mises calculus to derive the canonical gradient $D^d(P)(\mathbf{o})$ of the functional $\Psi^d(P)$ for a fixed $d \in \mathcal{D}_n$. This canonical gradient can be found in terms of the influence function of its square $\Phi^d(P) = \{\Psi^d(P)\}^2$, and using the fact that the tangent space is the whole of $L_0^2(P)$ in this nonparametric setting. Let $P_\epsilon = (1 - \epsilon)P + \epsilon\delta_{\mathbf{o}}$, where $\epsilon \in [0, 1]$ and $\delta_{\mathbf{o}}$ is the Dirac measure

at the point $\mathbf{o} = (\mathbf{x}^T, \mathbf{y}^T)^T$. When $\Psi^d(P) > 0$, we have

$$D^d(P)(\mathbf{o}) = \left. \frac{d\Psi^d(P_\epsilon)}{d\epsilon} \right|_{\epsilon=0} = \frac{1}{2\Psi^d(P)} \left. \frac{d\Phi^d(P_\epsilon)}{d\epsilon} \right|_{\epsilon=0} \quad (4)$$

where

$$\begin{aligned} \left. \frac{d\Phi^d(P_\epsilon)}{d\epsilon} \right|_{\epsilon=0} &= -\{\mathbf{x}_K - E_P(\mathbf{X}_K)\}^T \Sigma_{\mathbf{X}_K}^{-1} \Sigma_{\mathbf{X}_K \mathbf{Y}_J} \Sigma_{\mathbf{Y}_J}^{-1} \Sigma_{\mathbf{Y}_J \mathbf{X}_K} \Sigma_{\mathbf{X}_K}^{-1} \{\mathbf{x}_K - E_P(\mathbf{X}_K)\} \\ &\quad -\{\mathbf{y}_J - E_P(\mathbf{Y}_J)\}^T \Sigma_{\mathbf{Y}_J}^{-1} \Sigma_{\mathbf{Y}_J \mathbf{X}_K} \Sigma_{\mathbf{X}_K}^{-1} \Sigma_{\mathbf{X}_K \mathbf{Y}_J} \Sigma_{\mathbf{Y}_J}^{-1} \{\mathbf{y}_J - E_P(\mathbf{Y}_J)\} \\ &\quad + 2\{\mathbf{y}_J - E_P(\mathbf{Y}_J)\}^T \Sigma_{\mathbf{Y}_J}^{-1} \Sigma_{\mathbf{Y}_J \mathbf{X}_K} \Sigma_{\mathbf{X}_K}^{-1} \{\mathbf{x}_K - E_P(\mathbf{X}_K)\}. \end{aligned} \quad (5)$$

The details are given in Appendix A.1, where we also show that $E_P\{D^d(P)(\mathbf{O})\} = 0$, so the influence function belongs to the tangent space $L_0^2(P)$ and is thus the efficient influence function.

A continuous extension of $D^d(P)(\mathbf{o})$ to the case $\Psi^d(P) = 0$ is obtained as follows. The matrix-valued parameter $\psi(P) = \Lambda \equiv \Lambda_{\mathbf{Y}_J \mathbf{X}_K}$ is pathwise differentiable, so when $\psi(P) = 0$ there exists a matrix \mathbf{G} (which we can take as the efficient influence function) of the same dimensions as Λ and having entries in $L_0^2(P)$ such that $\psi(P_t)/t \rightarrow \langle \mathbf{G}, k \rangle$ as $t \rightarrow 0$ for any smooth one-dimensional parametric sub-model $\{P_t, t \in [0, 1]\}$ with score function $k \in L_0^2(P)$ at $t = 0$. Here the inner product notation in $\langle \mathbf{G}, k \rangle$ is understood to be applied entry-wise to \mathbf{G} . Writing $\Lambda_t \equiv \psi(P_t)$, and arranging that it does not vanish at any t apart from $t = 0$, it follows that $\Lambda_t / \|\Lambda_t\|_F \rightarrow \langle \mathbf{G}, k \rangle / \|\langle \mathbf{G}, k \rangle\|_F \equiv \mathbf{L}$ in Frobenius norm as $t \rightarrow 0$. It is then easily checked that for each fixed \mathbf{o} ,

$$D^d(P)(\mathbf{o}) \equiv \lim_{t \rightarrow 0} D^d(P_t)(\mathbf{o}) = \{\mathbf{y}_J - E_P(\mathbf{Y}_J)\}^T \Sigma_{\mathbf{Y}_J}^{-1/2} \mathbf{L} \Sigma_{\mathbf{X}_K}^{-1/2} \{\mathbf{x}_K - E_P(\mathbf{X}_K)\}, \quad (6)$$

providing the canonical gradient of $\Psi^d(P)$ when $\Psi^d(P) = 0$.

For univariate X and Y , the functional $P \mapsto \text{corr}_P(X, Y)$ has canonical gradient

$$\frac{\{x - E_P(X)\}\{y - E_P(Y)\}}{\sqrt{\text{var}(X)\text{var}(Y)}} - \frac{\text{corr}(X, Y)}{2\text{var}(X)} \{x - E_P(X)\}^2 - \frac{\text{corr}(X, Y)}{2\text{var}(Y)} \{y - E_P(Y)\}^2,$$

a result due to Colin Mallows (Devlin et al., 1975). When $\text{corr}(X, Y) = 0$ the last two terms above drop out, and the expression agrees with the canonical gradient of $\Psi^d(P)$ in (6), since $\mathbf{L} = 1$ in this case. In the multivariate case, the entries of the matrix \mathbf{L} are nuisance parameters that are absent in the univariate case.

The nuisance parameters in \mathbf{L} vary with d and the score function k , indicating the presence of non-regularity in the root-Pillai trace at zero, as the underlying k is not identifiable (it plays the role of a local parameter). When target parameters take values on the boundary of their parameter space (zero is on the boundary in our case), non-regularity is known to cause unstable asymptotics, such as inconsistency of the bootstrap, even in the simple example of a population mean restricted to be non-negative (Andrews, 2000). That is, dependence of a canonical gradient (or efficient influence function) on an arbitrary score function implies unstable behavior of the estimator, especially in small samples. This form of non-regularity is present in dimensions $p \geq 2$ and $q \geq 2$ (even without selection of $d \in \mathcal{D}_n$), but not in the case of univariate X and Y since the parameter space for the correlation coefficient is taken as the open interval $(-1, 1)$, which has no boundary.

This boundary type of non-regularity is distinct from the post-selection type of non-regularity noted by McKeague and Qian (2015, Section 2) in the case $p \geq 2$ and $q = 1$, in which the asymptotic distribution of the maximal absolute sample correlation is discontinuous at $\tau_{\max} = 0$. This type of non-regularity occurs in the present setting with the sample estimator of τ_{\max} given by

$$\widehat{\tau}_{\text{samp}} = \max_{|\mathcal{K}| \leq s_x, |\mathcal{J}| \leq s_y} \|\mathbf{C}_{\mathbf{Y}_{\mathcal{J}} \mathbf{X}_{\mathcal{K}}}\|_F = \max_{|\mathcal{K}| = s_x, |\mathcal{J}| = s_y} \|\mathbf{C}_{\mathbf{Y}_{\mathcal{J}} \mathbf{X}_{\mathcal{K}}}\|_F, \quad (7)$$

where $\mathbf{Y}_{\mathcal{J}} \in \mathbb{R}^{s_y}$ and $\mathbf{X}_{\mathcal{K}} \in \mathbb{R}^{s_x}$ are the selected variables. Here the second equality is a direct consequence of Lemma 1 in the sequel. It is challenging to use the estimator $\widehat{\tau}_{\text{samp}}$ as a test statistic for the global null hypothesis that $\tau_{\max} = 0$ because of the discontinuity in its asymptotic distribution at the null, but the stabilized one-step estimator $\widehat{\tau}_{\max}$ introduced below avoids this difficulty.

Curiously, the boundary-type of non-regularity does not arise with the Pillai trace itself, since its canonical gradient (5) does not depend on any score function k ; an intuitive explanation is that by squaring the root-Pillai trace, the non-regularity is smoothed out at zero. However, this squaring has the effect of causing severe bias in the sampling distribution of the stabilized one-step estimator of τ_{\max}^2 , especially when τ_{\max} is small and in small samples (see Figures 3 and 4 in Section 4.2). This problem does not arise with $\widehat{\tau}_{\max}$, hence our focus in the sequel on the root-Pillai trace.

Many authors have studied hypothesis testing problems in which a nuisance parameter is only identifiable under the alternative (e.g., Davies, 1977, 1987, 2002; Hansen, 1996). Here we encounter the situation where nuisance parameters appear only in the null, so calibration of the test

statistic may potentially depend on \mathbf{L} . Leeb and Pötscher (2017) have studied a post-selection calibration method that uses estimates of such nuisance parameters, but, as we will see, our approach leads to an asymptotically pivotal estimator of τ_{\max} without the need to estimate \mathbf{L} .

2.3 Stabilized one-step estimator

In this section we develop the stabilized one-step estimator for the target parameter τ_{\max} in terms of the canonical gradient $D^d(P)$, which will be estimated by plugging-in empirical distributions in place of P in (4). The data are first randomly ordered and we consider subsamples consisting of the first j observations for $j = \ell_n, \dots, n-1$, where $\{\ell_n\}$ is some positive integer sequence such that both ℓ_n and $n - \ell_n$ tend to infinity. In practice, we recommend randomly ordering the data say $K = 10$ times, and then combining the K confidence intervals by averaging (for more details see the real data example). Let P_j be the empirical distribution of the first j observations. The following procedure is a version of the construction of the stabilized one-step estimator in Luedtke and van der Laan (2018).

For each $j = \ell_n, \dots, n-1$, compute the following quantities:

1. The selected subsets of variables $d_{nj} = (\widehat{\mathcal{K}}, \widehat{\mathcal{J}})$ given by

$$d_{nj} \equiv \operatorname{argmax}_{d \in \mathcal{D}_n} \Psi^d(P_j) = \operatorname{argmax}_{|\mathcal{K}|=s_x, |\mathcal{J}|=s_y} \|\mathbf{C}_{\mathbf{X}_{\mathcal{K}}\mathbf{Y}_{\mathcal{J}}}(P_j)\|_F. \quad (8)$$

2. The corresponding maximum $\Psi^{d_{nj}}(P_j) = \|\mathbf{C}_{\mathbf{X}_{\widehat{\mathcal{K}}}\mathbf{Y}_{\widehat{\mathcal{J}}}}(P_j)\|_F$ and $\widehat{D}_j(\mathbf{O}_{j+1}) \equiv D^{d_{nj}}(P_j)(\mathbf{O}_{j+1})$ using the canonical gradient given by (4) and (5) with $P = P_j$.

3. An estimate of the variance of $\widehat{D}_j(\mathbf{O}_{j+1})$:

$$\widehat{\sigma}_j^2 = \frac{1}{j} \sum_{i=1}^j \left\{ \widehat{D}_j(\mathbf{O}_i) - \frac{1}{j} \sum_{m=1}^j \widehat{D}_j(\mathbf{O}_m) \right\}^2.$$

4. Weights $w_j = \bar{\sigma}_n / \widehat{\sigma}_j$, where $\bar{\sigma}_n = \left(\frac{1}{n - \ell_n} \sum_{j=\ell_n}^{n-1} \widehat{\sigma}_j^{-1} \right)^{-1}$ is the harmonic mean of the $\widehat{\sigma}_j$, $j = \ell_n, \dots, n-1$.

The stabilized one-step estimator for the target parameter τ_{\max} is then given by

$$\widehat{\tau}_{\max} = \frac{1}{n - \ell_n} \sum_{j=\ell_n}^{n-1} w_j \left\{ \Psi^{d_{nj}}(P_j) + \widehat{D}_j(\mathbf{O}_{j+1}) \right\}, \quad (9)$$

and an asymptotic $100(1 - \alpha)\%$ Wald-type confidence interval for τ_{\max} is

$$[\text{LB}_n, \text{UB}_n] = \left[\hat{\tau}_{\max} - z_{\alpha/2} \frac{\bar{\sigma}_n}{\sqrt{n - \ell_n}}, \hat{\tau}_{\max} + z_{\alpha/2} \frac{\bar{\sigma}_n}{\sqrt{n - \ell_n}} \right], \quad (10)$$

where $z_{\alpha/2}$ is the upper $\alpha/2$ -quantile of standard normal. For an α -level test of $\tau_{\max} = 0$ versus $\tau_{\max} > 0$, reject the null hypothesis $\tau_{\max} = 0$ if the lower bound of the $100(1 - 2\alpha)\%$ confidence interval exceeds 0. The estimator $\hat{\tau}_{\max}$ is a weighted version of the ‘‘online’’ one-step estimator introduced by van der Laan and Lendle (2014), where in our case $\Psi^{d_{nj}}(P_j)$ is improved using its estimated canonical gradient evaluated at a new observation.

Recursive properties of the algorithm allow considerable speed-up in the computation (see Section A.3 of the Appendix). Further, when the sample size n is large, we follow Luedtke and van der Laan (2018)’s suggestion of speeding up the $(n - \ell_n)$ updates by restricting the sample stream over $j = \ell_n, \dots, n - 1$ to only involve increments in j of size $C \geq 2$. The asymptotic properties of the stabilized one-step estimator are not affected by C . In our experience, the results are insensitive to the choice of C , provided n is sufficiently large relative to C . We fixed $C = 20$ and $\ell_n = \lceil n/2 \rceil$ in our numerical studies. Methods for estimating the number of non-zero canonical correlation coefficients K have been extensively studied in the signal processing literature (e.g., Song et al., 2016; Seghouane and Shokouhi, 2019), and these can be used to provide a lower bound on the choice of s_x and s_y . In practice, however, we recommend specifying s_x and s_y via a graphical inspection of the increments in the sample Pillai trace as the sparsity levels increase, see Figure 1 in Section 3.

2.4 Asymptotic results

We assume that each variable $X_k, k = 1, \dots, p$, or $Y_j, j = 1, \dots, q$, is bounded within $[-1, 1]$, and that the canonical gradient of $\Psi^d(P)$ satisfies

$$\inf_{n \geq 2} \min_{d \in \mathcal{D}_n} \text{var}_P \{D^d(P)(\mathbf{O})\} \geq \gamma, \quad (11)$$

for some constant $\gamma > 0$. This condition is mild in view of (4) and (6), and is imposed to ensure a non-degenerate asymptotic distribution for the one-step estimator, as needed to form non-trivial confidence intervals for τ_{\max} . To ensure that the canonical gradient is uniformly bounded for all d ,

we also assume that, for some $\delta > 0$,

$$\sup_{d \in \mathcal{D}_n} \max\{\|\Sigma_{\mathbf{X}_{\mathcal{K}}}^{-1}\|, \|\Sigma_{\mathbf{Y}_{\mathcal{J}}}^{-1}\|\} < \delta^{-1}, \quad (12)$$

where $\|\mathbf{M}\|$ denotes the largest singular value of matrix \mathbf{M} (or the operator norm). This mild condition means that the smallest eigenvalue of $\Sigma_{\mathbf{X}_{\mathcal{K}}}$ (or $\Sigma_{\mathbf{Y}_{\mathcal{J}}}$) is greater than some constant δ . We treat δ, γ and $s = s_x = s_y$ as fixed, and thus omit the dependence on δ, γ and s in the asymptotic statements. On the other hand, we allow both dimensions p and q to grow with the sample size n . When $p = p_n \rightarrow \infty$ and $q = q_n \rightarrow \infty$, it suffices to assume that $\log(p + q)/\sqrt{n} \rightarrow 0$. More generally, define $\beta_n^2 = n^{-1/2} \cdot \log \max\{n, p, q\}$, let for some $\epsilon \in (0, 2)$

$$\ell_n = \max\left\{(\log \max(n, p, q))^{1+\epsilon}, n \exp(-\beta_n^{-2+\epsilon})\right\} \quad (13)$$

and assume

$$\frac{\log \max(n, p, q)}{\ell_n} \rightarrow 0, \quad \beta_n^2 \log \frac{n}{\ell_n} \rightarrow 0, \quad \limsup_{n \rightarrow \infty} \frac{\ell_n}{n} < 1. \quad (14)$$

For the estimation procedure described in Section 2.3, we then have the following result on the lower bound of the confidence interval.

Theorem 1 (Tightness of the lower bound). *Under conditions (11), (12) and (14), for any sequence $t_n \rightarrow \infty$, $\Psi_n(P) < \text{LB}_n + t_n n^{-1/4} \beta_n$ with probability approaching 1.*

Theorem 1 establishes the validity and tightness of the lower bound of the confidence interval for τ_{\max} . This result immediately implies the asymptotic validity of our testing procedure for $H_0 : \tau_{\max} = 0$ versus $H_a : \tau_{\max} > 0$. To establish the upper bound, we further assume the following margin condition: for some sequence $t_n \rightarrow \infty$, there exists a sequence of nonempty subsets $\mathcal{D}_n^* \subseteq \mathcal{D}_n$ such that, for all n ,

$$\sup_{d_1, d_2 \in \mathcal{D}_n^*} \{\Psi^{d_1}(P) - \Psi^{d_2}(P)\} = o(n^{-1/2}), \quad \inf_{d \in \mathcal{D}_n^*} \Psi^d(P) - \sup_{d \in \mathcal{D}_n \setminus \mathcal{D}_n^*} \Psi^d(P) \geq t_n n^{-1/2} \beta_n. \quad (15)$$

Theorem 2 (Validity of the upper bound). *Under the same conditions as in Theorem 1, if we further assume (15) or $\Psi_n(P) = 0$ for all n , then $\text{LB}_n \leq \Psi_n(P) \leq \text{UB}_n$ with probability approaching $1 - \alpha$.*

These theorems, as well as their technical assumptions, are generalizations of Theorems 2 and 3 of Luedtke and van der Laan (2018) and specialize to their results when $s_x = 1$ and $q = s_y = 1$

in connection with the univariate maximal correlation setting of McKeague and Qian (2015). The extension to the general multivariate analysis of variance setting (i.e., the maximal Pillai trace) is highly non-trivial because of extra challenges that arises when analyzing the canonical gradient (given by (4) and (5)), and specifically in bounding its second-order remainder term (see the Supplementary Materials).

3 Greedy search for maximal Pillai trace

3.1 Algorithm

When computing the stabilized one-step estimator, the computationally most costly part is the optimization in (8). To obtain d_{nj} , we need to search over subsets \mathcal{K} of size s_x and, similarly, over subsets \mathcal{J} of size s_y . This means a search over $\binom{p}{s_x} \binom{q}{s_y}$ possible combinations, which is computationally too expensive when p and q are large. In some applications, there may be a neighborhood structure that can be exploited to reduce computational expense. For example, restricting to neighborhoods of the form $\mathcal{K} = \{1, \dots, s_x\}, \{2, \dots, s_x + 1\}, \dots$, gives $p - s_x + 1$ possible subsets in total. Then in total, we only have to compute the Pillai trace of $(p - s_x + 1)(q - s_y + 1)$ combinations.

Nevertheless, in general there is a need to speed up the first step of the computation of the stabilized one-step estimator given in the previous section. To that end, we introduce the scalable greedy search in Algorithm 1 to (approximately) maximize the Pillai trace $\|\mathbf{C}_{\mathbf{X}_{\mathcal{K}}\mathbf{Y}_{\mathcal{J}}}\|_F^2$ over $|\mathcal{K}| = s_x$ and $|\mathcal{J}| = s_y$.

This algorithm is much more efficient than a full combinatorial search. For all $j \notin \mathcal{J}$ and $k \notin \mathcal{K}$, we consider the increments in the Pillai trace $\|\mathbf{C}_{\mathbf{Y}_{\mathcal{J}}\mathbf{X}_{\mathcal{K}}}\|_F^2$ by replacing \mathcal{J} with $\mathcal{J} \cup \{j\}$ and replacing \mathcal{K} with $\mathcal{K} \cup \{k\}$. Let $E_{j|\mathcal{J}} = Y_j - \mathbb{E}(Y_j) - \Sigma_{Y_j\mathbf{Y}_{\mathcal{J}}}\Sigma_{\mathbf{Y}_{\mathcal{J}}}^{-1}\{\mathbf{Y}_{\mathcal{J}} - \mathbb{E}(\mathbf{Y}_{\mathcal{J}})\}$ be the residual of Y_j regressed on $\mathbf{Y}_{\mathcal{J}}$, and similarly, $R_{k|\mathcal{K}}$ be the residual of X_k regressed on $\mathbf{X}_{\mathcal{K}}$. The sample versions of $E_{j|\mathcal{J}}$ and $R_{k|\mathcal{K}}$ are obtained using ordinary least squares and then plugged in the calculation of $\mathbf{C}_{E_{j|\mathcal{J}}\mathbf{X}_{\mathcal{K}}}$ and $\mathbf{C}_{R_{k|\mathcal{K}}\mathbf{Y}_{\mathcal{J}}}$. This leads to the following result.

Lemma 1. *Assume that $\mathbf{S}_{\mathbf{Y}_{\mathcal{J}}} > 0$, $\mathbf{S}_{\mathbf{X}_{\mathcal{K}}} > 0$ and $n > \max(s_x, s_y) + 1$. Then*

$$\|\mathbf{C}_{\mathbf{Y}_{\mathcal{J} \cup \{j\}}\mathbf{X}_{\mathcal{K}}}\|_F^2 = \|\mathbf{C}_{\mathbf{Y}_{\mathcal{J}}\mathbf{X}_{\mathcal{K}}}\|_F^2 + \|\mathbf{C}_{E_{j|\mathcal{J}}\mathbf{X}_{\mathcal{K}}}\|_F^2, \quad (16)$$

$$\|\mathbf{C}_{\mathbf{Y}_{\mathcal{J}}\mathbf{X}_{\mathcal{K} \cup \{k\}}}\|_F^2 = \|\mathbf{C}_{\mathbf{Y}_{\mathcal{J}}\mathbf{X}_{\mathcal{K}}}\|_F^2 + \|\mathbf{C}_{\mathbf{Y}_{\mathcal{J}}R_{k|\mathcal{K}}}\|_F^2, \quad (17)$$

$$\|\mathbf{C}_{\mathbf{Y}_{\mathcal{J} \cup \{j\}}\mathbf{X}_{\mathcal{K} \cup \{k\}}}\|_F^2 = \|\mathbf{C}_{\mathbf{Y}_{\mathcal{J}}\mathbf{X}_{\mathcal{K}}}\|_F^2 + \|\mathbf{C}_{E_{j|\mathcal{J}}\mathbf{X}_{\mathcal{K}}}\|_F^2 + \|\mathbf{C}_{\mathbf{Y}_{\mathcal{J}}R_{k|\mathcal{K}}}\|_F^2 + \|\mathbf{C}_{E_{j|\mathcal{J}}R_{k|\mathcal{K}}}\|_F^2. \quad (18)$$

Algorithm 1 Greedy search

1. Initialize $\mathcal{J} = \{j\}$ and $\mathcal{K} = \{k\}$, where (j, k) maximizes $\|\mathbf{C}_{Y_j X_k}\|_F^2 = \widehat{\text{corr}}^2(Y_j, X_k)$.
 2. Selection over $j \notin \mathcal{J}$ and $k \notin \mathcal{K}$.
 - (a) If $|\mathcal{J}| < s_y$ and $|\mathcal{K}| < s_x$, find $j \notin \mathcal{J}$ and $k \notin \mathcal{K}$ that maximizes $\delta_j^{\mathcal{J}, \mathcal{K}} \equiv \|\mathbf{C}_{E_{j|\mathcal{J}} \mathbf{x}_{\mathcal{K}}}\|_F^2$ and $\gamma_k^{\mathcal{J}, \mathcal{K}} \equiv \|\mathbf{C}_{\mathbf{Y}_{\mathcal{J}} R_{k|\mathcal{K}}}\|_F^2$, respectively. Then update $\mathcal{J} \rightarrow \mathcal{J} \cup j$ if $\max_{j \notin \mathcal{J}} \delta_j^{\mathcal{J}, \mathcal{K}} > \max_{k \notin \mathcal{K}} \gamma_k^{\mathcal{J}, \mathcal{K}}$, otherwise update $\mathcal{K} \rightarrow \mathcal{K} \cup k$.
 - (b) If $|\mathcal{J}| < s_y$ and $|\mathcal{K}| = s_x$, update $\mathcal{J} \rightarrow \mathcal{J} \cup j$ where $j \notin \mathcal{J}$ maximizes $\delta_j^{\mathcal{J}, \mathcal{K}}$.
 - (c) If $|\mathcal{J}| = s_y$ and $|\mathcal{K}| < s_x$, update $\mathcal{K} \rightarrow \mathcal{K} \cup k$ where $k \notin \mathcal{K}$ maximizes $\gamma_k^{\mathcal{J}, \mathcal{K}}$.
 3. Update the Pillai trace based on the increment given in Lemma 1.
 4. Repeat Steps 2 and 3 until $|\mathcal{J}| = s_y$ and $|\mathcal{K}| = s_x$.
 5. Output: $\widehat{\mathcal{J}}, \widehat{\mathcal{K}}$ and $\|\mathbf{C}_{\mathbf{Y}_{\widehat{\mathcal{J}}} \mathbf{x}_{\widehat{\mathcal{K}}}}\|_F^2$ or $\|\mathbf{C}_{\mathbf{Y}_{\widehat{\mathcal{J}}} \mathbf{x}_{\widehat{\mathcal{K}}}}\|_F$.
-

This result gives the increment in the Pillai trace when including an additional variable in either \mathbf{X} or \mathbf{Y} , or both, and allows us to implement the greedy search via forward stepwise selection in Algorithm 1. Another implication of Lemma 1 is that, as we mentioned earlier in equation (7), $\max_{|\mathcal{K}|=s_x, |\mathcal{J}|=s_y} \|\mathbf{C}_{\mathbf{Y}_{\mathcal{J}} \mathbf{x}_{\mathcal{K}}}\|_F^2 = \max_{|\mathcal{K}| \leq s_x, |\mathcal{J}| \leq s_y} \|\mathbf{C}_{\mathbf{Y}_{\mathcal{J}} \mathbf{x}_{\mathcal{K}}}\|_F^2$. This means that even if one uses the full greedy search over $\{|\mathcal{K}| \leq s_x, |\mathcal{J}| \leq s_y\}$, our result narrows down the search to $\{|\mathcal{K}| = s_x, |\mathcal{J}| = s_y\}$.

An alternative version of Algorithm 1 involves maximizing over increments of the root-Pillai trace, which by (16) in Lemma 1 can be expressed in terms of increments of the Pillai trace as

$$\|\mathbf{C}_{\mathbf{Y}_{\mathcal{J} \cup \{j\}} \mathbf{x}_{\mathcal{K}}}\|_F - \|\mathbf{C}_{\mathbf{Y}_{\mathcal{J}} \mathbf{x}_{\mathcal{K}}}\|_F = \|\mathbf{C}_{E_{j|\mathcal{J}} \mathbf{x}_{\mathcal{K}}}\|_F / \left(\sqrt{\|\mathbf{C}_{\mathbf{Y}_{\mathcal{J}} \mathbf{x}_{\mathcal{K}}}\|_F^2 + \|\mathbf{C}_{E_{j|\mathcal{J}} \mathbf{x}_{\mathcal{K}}}\|_F^2} + \|\mathbf{C}_{\mathbf{Y}_{\mathcal{J}} \mathbf{x}_{\mathcal{K}}}\|_F \right).$$

The above expression is an increasing function of $\|\mathbf{C}_{E_{j|\mathcal{J}} \mathbf{x}_{\mathcal{K}}}\|_F^2$, so the same index j must maximize both of these increments and the alternative version of Algorithm 1 is therefore equivalent.

This greedy search algorithm is related to one proposed by Wiesel et al. (2008), which was designed for sparse maximization of the sample version of the leading canonical correlation coefficient ρ . However, we have two important advantages. First, due to Lemma 1, we are able to maximize and update *exact* increments in the Pillai trace, namely $\|\mathbf{C}_{E_{j|\mathcal{J}} \mathbf{x}_{\mathcal{K}}}\|_F^2$ and $\|\mathbf{C}_{\mathbf{Y}_{\mathcal{J}} R_{k|\mathcal{K}}}\|_F^2$, whereas in Wiesel et al. (2008) the exact increments in ρ are not available and the maximization is carried out on lower bounds of the increments. Second, to obtain the maximal canonical

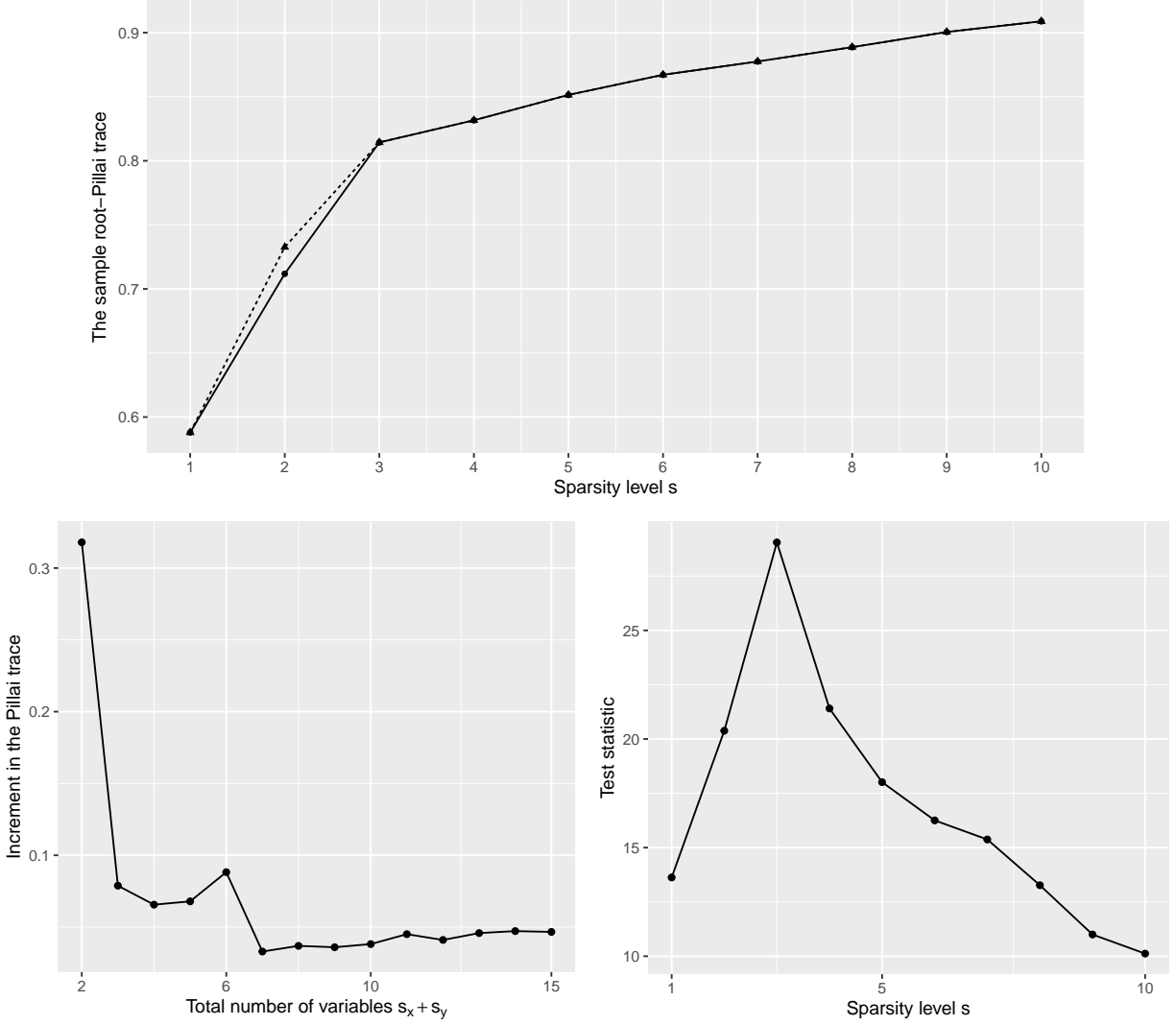


Figure 1: Results based on single samples generated under Model A1 with $n = 500$, $s_x^* = s_y^* = 3$, $\tau_{\max} = 0.8$. Top panel: values of $\hat{\tau}_{\text{samp}}$ from a full search (dotted line) and a greedy search (solid line) as the sparsity level $s = s_x = s_y$ varies from 1–10, for $p = q = 10$. Bottom left: scree plot of the increment in the sample Pillai trace, $\|\mathbf{C}_{E_j|\mathcal{J}}\mathbf{x}_\kappa\|_F^2$ or $\|\mathbf{C}_{\mathbf{Y}_{\mathcal{J}}R_k|\mathcal{K}}\|_F^2$, when adding one variable at a time in the greedy search, for $p = q = 5000$. Bottom right: corresponding values of the studentized $\hat{\tau}_{\max}$ (test statistic for $\tau_{\max} = 0$) as a function of s .

correlation, the CCA directions α and β also need to be updated at each step of including an additional variable, while the update for the Pillai trace is automatically obtained by the equations in Lemma 1 using linear regression residuals. Therefore, our approach is both more accurate and computationally more efficient than Wiesel et al. (2008)’s greedy search algorithm.

The top panel of Figure 1 gives the results from a toy example showing that the proposed greedy algorithm for finding the maximal sample root-Pillai trace under varying sparsity constraints pro-

vides almost perfect agreement with the full search. The data were generated from Model A1 used in the simulation study (in Section 4), with $p = q = 10$, the true numbers of active variables $s_x^* = s_y^* = 3$, $\tau_{\max} = 0.8$, the true number of non-zero canonical correlations $K = 1$, and $n = 500$. The result of the greedy search agrees with the full search at all sparsity levels except at $s = s_x = s_y = 2$.

Algorithm 1 can naturally be modified so as not to require pre-specified sparsity levels. In step 2, either j or k is added, whichever gives the larger increment in the Pillai trace. The algorithm can then be terminated in Step 4 when the increment is smaller than some given tolerance, say 0.05 or 0.01. The bottom-left panel of Figure 1 shows the successive increments in the sample Pillai trace when adding one variable at a time (either X_k or Y_j), using the same simulation model as the first panel except with $p = q = 5000$. This plot is analogous to the scree plot used in principal component analysis and factor analysis, providing intuition and graphical diagnostics for how sparse the true model might be. It is clear from the plot that $s_x + s_y = 6$ gives the most reasonable terminating point; also, at that point we have $s_x = s_y = 3$ (not shown in the plot), agreeing with the true numbers of active variables. The bottom-right panel of Figure 1 shows the corresponding values of the studentized $\hat{\tau}_{\max}$ used as the test statistic for the proposed test. As the sparsity level s increases, the test statistic monotonically increases until s reaches the true value $s_x^* = s_y^* = 3$, but the accuracy of the sample coherence matrix $\mathbf{C}_{\mathbf{X}_{\mathcal{K}}\mathbf{Y}_{\mathcal{J}}}$ used in the test statistic decreases as its dimension ($s_x \times s_y$) grows, causing a decrease in power at larger values of s . In our experience, the proposed test performs well for relatively small sparsity levels, as in this simulation example, but degrades when s_x^* and s_y^* become large (say $s_x^* = s_y^* = 20$).

3.2 Submodularity

To gain some further insight into the performance the proposed greedy search algorithm, we show in a simulation example that the root-Pillai trace comes close to satisfying the submodular property (which, if true, would give a guarantee of finding the maximum to within a factor of $1/e$). Maximization of the root-Pillai trace over \mathcal{K} and \mathcal{J} is a discrete combinatorial optimization problem for a set function $f: 2^V \mapsto \mathbb{R}$, where the finite set $V = \{1, \dots, p\} \times \{1, \dots, q\}$ and the utility function is $f(S) = \|\mathbf{C}_{\mathbf{X}_{\mathcal{K}}\mathbf{Y}_{\mathcal{J}}}\|_F$ for $S = (\mathcal{J}, \mathcal{K}) \subseteq V$. Submodularity in set functions is the discrete analogy of convexity in continuous functions. Fast greedy algorithms with theoretical guar-

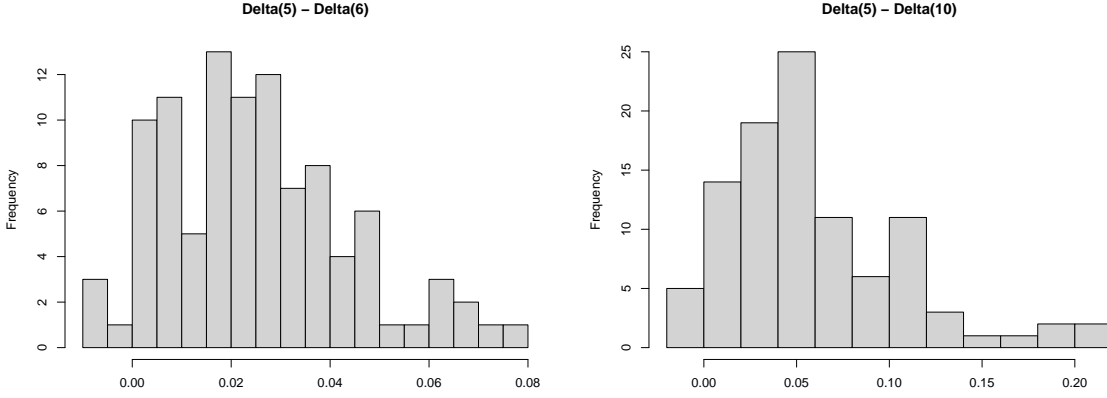


Figure 2: Histograms used for checking submodularity of the root-Pillai trace as a function of $S = (\mathcal{J}, \mathcal{K})$ for the GBM data set. The plotted values of $\Delta(e_i | S_1) - \Delta(e_i | S_2)$ should be non-negative if the function is submodular. The histograms are based on 100 randomly sampled elements $e_i \notin S_2$. The set S_2 is randomly chosen with $|\mathcal{K}| = |\mathcal{J}| = 6$ on the left, and with $|\mathcal{K}| = |\mathcal{J}| = 10$ on the right. For $S_1 \subset S_2$ we take the first 5 elements of S_2 .

antees have been developed for submodular function maximization (see Nemhauser and Wolsey, 1978; Krause and Golovin, 2014; Khim et al., 2016, for example), when the utility function is also monotonic. Specifically, the set function f is monotonic if for any two sets $S_1 \subseteq S_2 \subseteq V$, we have $f(S_1) \leq f(S_2)$. Based on Lemma 1, it is not difficult to see that $f(S) = \|\mathbf{C}_{\mathbf{X}_{\mathcal{K}} \mathbf{Y}_{\mathcal{J}}}\|_F$ is monotonic.

We now briefly review the definition of submodularity and then numerically demonstrate that our set function f can be close to submodular, although not exactly so. A key concept related to submodularity is the discrete derivative. The discrete derivative of f at S with respect to a new element $e \in V$ is defined as $\Delta(e | S) = f(S \cup \{e\}) - f(S)$. Then f is called submodular if, for any $S_1 \subseteq S_2 \subset V$ and $e \in V \setminus S_2$, we have $\Delta(e | S_1) \geq \Delta(e | S_2)$. We consider a simple numerical experiment using the real data in Section 5, where $(p, q, n) = (1000, 534, 397)$. First, we randomly sampled $S_2 \subset V$ with size $s_x = s_y = 6$ (or 10) and defined the first 5 elements in S_2 to be S_1 . Then we computed the histogram of the differences $\Delta(e_i | S_1) - \Delta(e_i | S_2)$ for 100 randomly selected elements $e_i \notin S_2$. The results displayed in Figure 2 indicate a close approximation to submodularity since there are very few negative values in each histogram. In contrast, the Pillai trace is readily seen to violate the submodular property: the scree plot in Figure 1 is not monotonically decreasing.

4 Simulation study

The sample size is fixed at $n = 500$, while we vary the dimensions of \mathbf{X} and \mathbf{Y} from $p = q = 10$ to $p = q = 5000$. We generated i.i.d. samples $(\mathbf{X}_i^T, \mathbf{Y}_i^T)^T \in \mathbb{R}^{p+q}$, $i = 1, \dots, n$, from a joint normal distribution with mean zero and covariance specified by

$$(\boldsymbol{\Sigma}_{\mathbf{X}})_{jl} = (\boldsymbol{\Sigma}_{\mathbf{Y}})_{jl} = \begin{cases} 0.5^{|j-l|}, & j, l \leq 100, \\ I(j = l), & \text{otherwise,} \end{cases} \quad \boldsymbol{\Sigma}_{\mathbf{XY}} = \boldsymbol{\Sigma}_{\mathbf{X}} \left(\sum_{k=1}^K \rho_k \boldsymbol{\alpha}_k \boldsymbol{\beta}_k^T \right) \boldsymbol{\Sigma}_{\mathbf{Y}}. \quad (19)$$

The above structured $\boldsymbol{\Sigma}_{\mathbf{XY}}$ is commonly used in the sparse CCA literature (e.g., Mai and Zhang, 2019), where K is the number of non-zero CCA coefficients, $\rho_k > 0$ is the k -th canonical correlation, $\boldsymbol{\alpha}_k$ and $\boldsymbol{\beta}_k$ are the corresponding sparse CCA directions that satisfy all the length, orthogonality and sparsity constraints. Also, the maximal canonical correlation coefficient $\rho = \rho_1$. Note that the number K is irrelevant in our estimation as we did not use that information. Under this simulation setting, the covariance matrices $\boldsymbol{\Sigma}_{\mathbf{X}}$, $\boldsymbol{\Sigma}_{\mathbf{Y}}$ and $\boldsymbol{\Sigma}_{\mathbf{XY}}$ are not sparse while the sparsity is imposed directly on each $\boldsymbol{\alpha}_k$ and $\boldsymbol{\beta}_k$. The nonzero elements in $\boldsymbol{\alpha}$ and $\boldsymbol{\beta}$ correspond to the active variables in \mathbf{X} and \mathbf{Y} , respectively. In our simulations, we have the symmetry in \mathbf{X} and \mathbf{Y} and thereby set $\boldsymbol{\alpha}_k = \boldsymbol{\beta}_k$, which implies $s_x^* = s_y^*$.

We consider three scenarios of the form (19). The first scenario is a model satisfying null hypothesis (Model N), where $\boldsymbol{\Sigma}_{\mathbf{XY}} = 0$, $K = 0$, $s_x^* = s_y^* = 0$, and we vary the prescribed sparsity levels $s_x = s_y = s \in \{1, 2, 3, 4\}$. The next two scenarios are alternative hypothesis models (Models A1 and A2), with the true numbers of active variables $s_x^* = s_y^* = 3$. Without loss of generality, the active variables are taken as the first three components of \mathbf{X} and \mathbf{Y} . Model A1 is the single pair CCA model with $K = 1$, so $\tau = \rho$. The SCCA direction $\boldsymbol{\alpha}_1 = \boldsymbol{\beta}_1$ is set as $\mathbf{v}_1 / \sqrt{\mathbf{v}_1^T \boldsymbol{\Sigma}_{\mathbf{X}} \mathbf{v}_1}$ to satisfy the length constraint, where $\mathbf{v}_1 = (1, 1, 1, 0, \dots, 0)^T$. For Model A2, a general SCCA model, we take the number of components $K = 3$ and set $(\rho_1, \rho_2, \rho_3) = (\tau, 2\tau, 3\tau) / \sqrt{14}$. The SCCA directions $\boldsymbol{\alpha}_k = \boldsymbol{\beta}_k$, $k = 1, 2, 3$, are set to have 1 in the k -th component and 0's elsewhere. Under the Models A1 and A2, we vary $\tau \in \{0.1, 0.2, 0.3, 0.4\}$ to study the effect of changes in the strength of the correlation.

4.1 Simulation results for hypothesis testing

We compared various methods (whenever they are applicable) for the 5%-level test of $\tau_{\max} = 0$ versus $\tau_{\max} > 0$: the proposed testing procedure using the stabilized one-step estimator (OS); the

p		Model N				Model A1				Model A2			
		$s = 1$	2	3	4	$\tau = 0.1$	0.2	0.3	0.4	$\tau = 0.1$	0.2	0.3	0.4
10	OS	0.066	0.056	0.050	0.064	0.124	0.546	0.950	1	0.098	0.448	0.894	0.998
	HC	0.122	0.530	0.542	0.532	0.802	0.980	1	1	0.734	0.960	1	1
	MF	0.050	0.050	0.050	0.050	0.096	0.368	0.860	0.996	0.104	0.388	0.888	0.998
	SF	0.984	0.952	0.930	0.894	0.962	0.998	1	1	0.984	1	1	1
	BF	0.050	0.004	0.004	0	0.020	0.312	0.936	1	0.016	0.254	0.846	1
30	OS	0.058	0.054	0.074	0.056	0.068	0.312	0.830	0.996	0.064	0.234	0.720	0.980
	HC	0.134	0.628	-	-	-	-	-	-	-	-	-	-
	MF	0.034	0.034	0.034	0.034	0.040	0.072	0.216	0.470	0.042	0.074	0.216	0.496
	BF	0.048	0.008	0.002	0	0.002	0.074	0.662	0.996	0.004	0.062	0.530	0.966
100	OS	0.054	0.072	0.070	0.080	0.074	0.190	0.660	0.982	0.058	0.136	0.588	0.946
	BF	0.046	0.010	0.002	0	0.002	0.018	0.366	0.962	0	0.024	0.304	0.906
1000	OS	0.066	0.056	0.050	0.064	0.066	0.076	0.274	0.866	0.072	0.074	0.334	0.838
	BF	0.046	0.010	0.002	0	0.002	0.002	0.072	0.664	0.002	0.002	0.068	0.646
5000	OS	0.082	0.068	0.072	0.066	0.072	0.076	0.154	0.670	0.066	0.072	0.174	0.732
	BF	0.052	0.002	0	0	0	0	0.016	0.330	0	0	0.016	0.428

Table 1: Simulation under the null Model N and the two alternative models A1 and A2. The reported numbers are the rejected proportion based on 500 replicated data sets for each of the simulation settings.

classical F-test for the Pillai trace without variable selection, as implemented in the `manova` R package (MF); naive application of the F-test on selected variables (SF), which comes without any adjustment for variable selection; the F-test on selected variables with Bonferroni correction (BF); and the Higher Criticism (HC) method (Donoho and Jin, 2004, 2015) based on p-values computed from the F-test for all $\binom{p}{s_x} \binom{q}{s_y}$ combinations of variables. The HC statistic was calculated following the procedure described in Donoho and Jin (2015, Sections 1.1 and 2.1) with the critical value calculated using the Gumbel distribution. For all methods that require variable selection (SF, BF, and OS), the variables were selected using Algorithm 1. All of the F-tests (MF/SF/BF) considered, as well as the HC procedure, are based on p-values for the MANOVA F-test that targets the Pillai trace, whereas our approach targets the root-Pillai trace. For the BF procedure, although we only used the F-statistic based on the $s_x + s_y$ variables selected from Algorithm 1, the Bonferroni

correction covers all $\binom{p}{s_x} \binom{q}{s_y}$ combinations of variables potentially involved in the F-test.

In Table 1, we report the proportion of rejections under each simulation setting, based on 500 simulation replications for each case. For the HC procedure, the total number of test statistics in one replication is $\binom{p}{s_x} \binom{q}{s_y}$. Therefore, it was only included for $p = 10$ and for $p = 30, s < 3$ scenarios, and was shown to have unsatisfactory type I error control. The MANOVA F-test (MF) worked well for low-dimensional null and alternative models, but is not applicable for $p > 30$. When $p \geq 30$, the F-test based on selected variables without any adjustment (SF) will always reject the null even under the null hypothesis (not show this in Table 1). This is not surprising as it fails to adjust for spurious correlations. The only two feasible methods for high-dimensional settings are seen to be the proposed test based on the stabilized one-step estimator (OS) and the Bonferroni corrected F-test (BF). Clearly, the proposed method has much better type I error control (under Model N) and much smaller type II error (under Models A1 and A2) than BF. Overall, the proposed OS testing procedure has adequately controlled the type I error around the nominal level $\alpha = 0.05$. Specifically, the type I error is always between 0.05 and 0.1 for all different $p \in \{10, 30, 100, 1000, 5000\}$ and $s \in \{1, 2, 3, 4\}$ combinations. Though the test procedure is asymptotically valid, the slightly anti-conservative results appear to be caused by the stabilized one-step estimation procedure at small sample size $j < n$. In contrast, HC and SF fail to control the type I error; BF is too conservative when $s > 1$; MF has the perfect type I error control only for $p = 10$, which verifies the superiority of the F-test over the Wald-type test in low-dimensional settings. It is also very encouraging to see that the proposed OS testing procedure is more powerful than BF and MF, even in low dimensions ($p = 10, 30$), and is able to detect weak signals (i.e. canonical correlations are no larger than 0.4 in all models) in very high dimensions ($p = 1000, 5000$).

4.2 Simulation results for parameter estimation

Although our theory and implementation are equally applicable to stabilized one-step estimators of τ_{\max} and τ_{\max}^2 , the empirical results for τ_{\max} are generally better than those of τ_{\max}^2 . Note that the stabilized one-step estimator of τ_{\max}^2 is not simply $\widehat{\tau}_{\max}^2$.

Histograms of the estimated τ_{\max} and τ_{\max}^2 from 500 independent samples (of size $n = 500$) under the null Model N are presented in Figure 3, where we vary $s_x = s_y = s \in \{1, 2, 3, 4\}$. The stabilized one-step estimates for τ_{\max} and τ_{\max}^2 are both seen to be approximately normal. For τ_{\max} ,

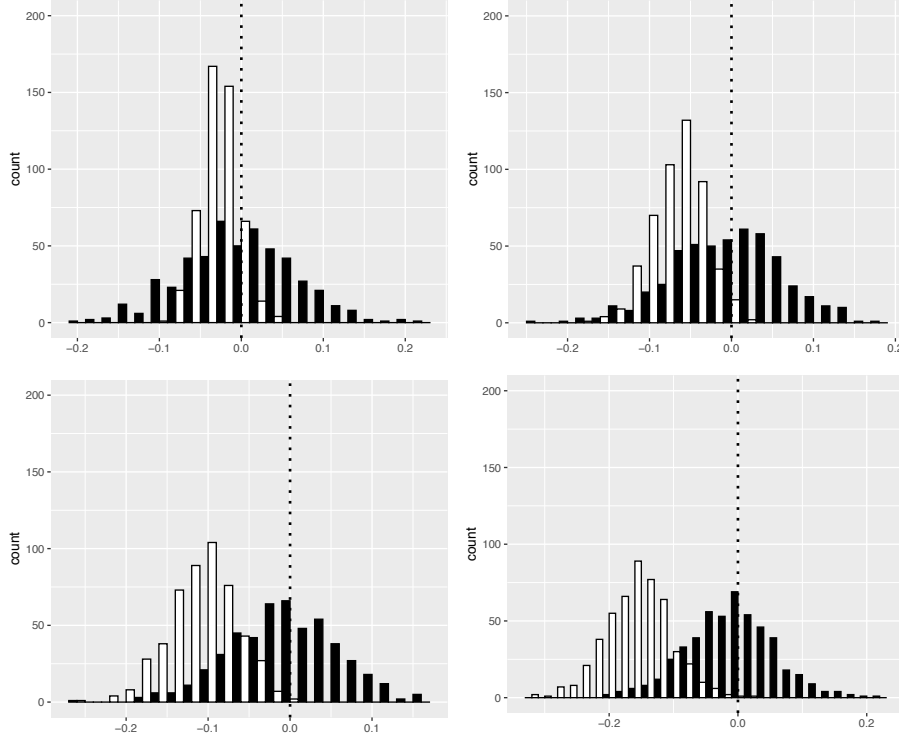


Figure 3: Histograms of $\hat{\tau}_{\max}$ (in black) under the null Model N based on 500 independent simulated data sets. The four panels, from top-left to bottom-right, correspond to the sparsity levels $s_x = s_y = s = 1, 2, 3$ and 4, respectively. The histograms in white are of the stabilized one-step estimator of τ_{\max}^2 , showing a negative bias that becomes increasingly pronounced as s increases.

the estimates are all centered around the truth, $\tau_{\max} = 0$, regardless of the choice of s . However, for τ_{\max}^2 , there is a severe under-estimation phenomenon, which becomes more pronounced as s increases. We think there are two factors contributing to this phenomenon. First, the number of parameters in $\mathbf{C}_{\mathbf{Y}_J \mathbf{X}_K}$ is s^2 . This requires a larger sample size n for the asymptotic properties to come into effect as s increases. Second, when the Pillai trace is close to zero, its absolute value is magnified by taking the square root, making it easier to estimate.

Under the alternative model (Model A1) with the correlation strength τ_{\max} varying from 0.2 to 0.8, the histograms of $\hat{\tau}_{\max}$ (again based on 500 independent samples of size $n = 500$) are given in the top panel of Figure 4. Recall that the true sparsity levels are $s_x^* = s_y^* = 3$ in this model. We also set $s_x = s_y = s = 3$. Although there is an issue of under-estimation for both τ_{\max} and τ_{\max}^2 when the signal is weak ($\tau_{\max} = 0.2$ and 0.4), there is a substantial improvement when the correlation is strong enough. The improvement is more pronounced in the histogram of $\hat{\tau}_{\max}$ compared with that of the stabilized one-step estimator of τ_{\max}^2 (bottom panel). It is worth noting

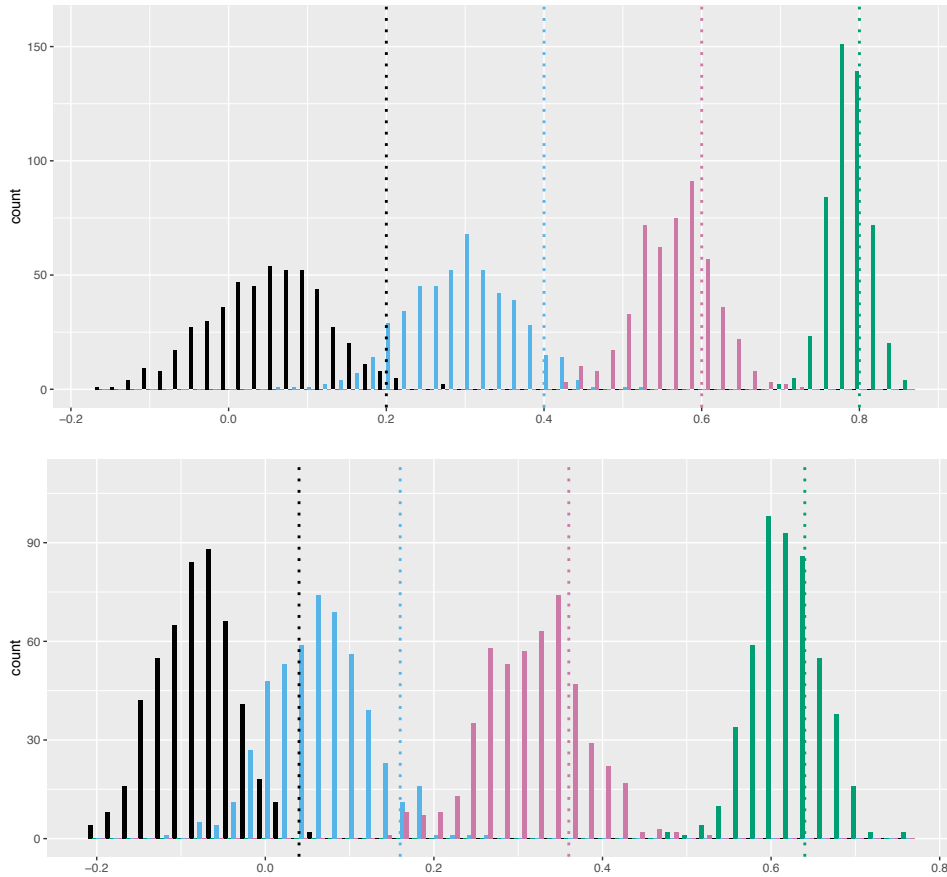


Figure 4: Histograms of the stabilized one-step estimators for τ_{\max} (top panel) and τ_{\max}^2 (bottom panel), under Model A1. In each plot, the four colored histograms going from left to right correspond to $\tau_{\max} = 0.2, 0.4, 0.6$ and 0.8 , respectively. The vertical dashed lines are the true values of the targeted parameters τ_{\max} (top) and τ_{\max}^2 (bottom).

that $\tau_{\max} = 0.8$ is still relatively weak correlation (e.g., the estimated τ_{\max} exceeds 1.5 in the real data example of Section 5), but both estimators worked well at $\tau_{\max} = 0.8$. An explanation for the under-estimation is that the stabilizing procedure tends to attenuate the estimates to some extent, at least in the neighborhood of $\tau_{\max} = 0$. However, as seen in Figure 3, the behavior of $\hat{\tau}_{\max}$ under the null model is unaffected by such attenuation, being approximately zero-mean normal.

5 Analysis of glioblastoma multiforme data

Glioblastoma multiforme (GBM) is a type of fast-growing brain tumor that is also the most common primary form of brain tumor in adults. Data were collected by The Cancer Genome Atlas project (TCGA Weinstein et al., 2013) on 490 patients with GBM, including data on $q = 534$

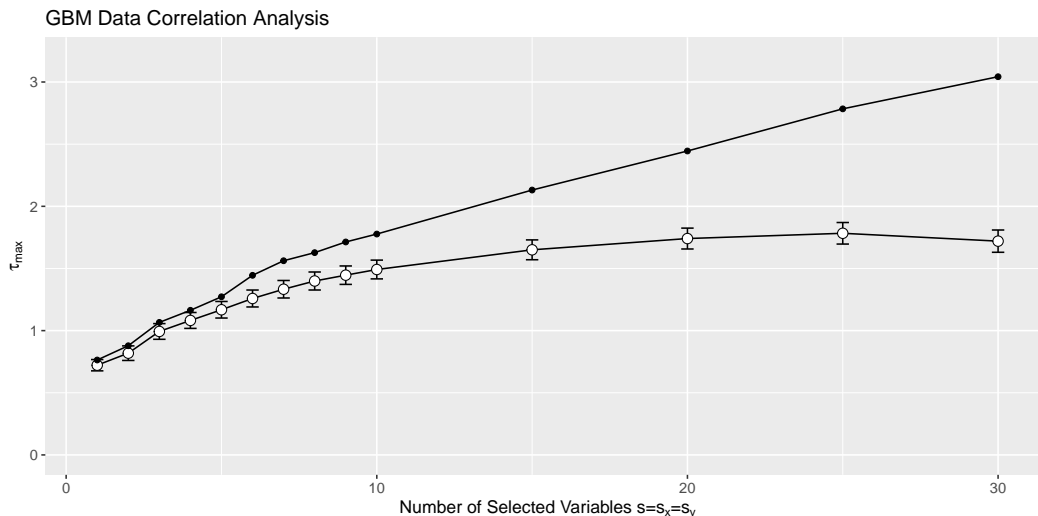


Figure 5: GBM data analysis. Estimates of the maximal root-Pillai trace τ_{max} are plotted against $s = s_x = s_y$ varying from 1–30, with the selected variables at each step found using Algorithm 1. The black dots are $\hat{\tau}_{\text{samp}}$ (without adjustment for post-selection), giving inflated estimates of τ_{max} . The white dots and associated 95% confidence intervals are based on the stabilized one-step estimator $\hat{\tau}_{\text{max}}$, with 10 random re-orderings and averaged point estimates and averaged lower/upper CI endpoints over these re-orderings.

microRNA expression and 17,472 gene expression measurements for each patient. It is of interest to find associations between microRNA and gene expression. Following previous studies (Wang, 2015; Molstad, 2019), we analyze the $p = 1000$ genes with the largest median absolute deviations in gene expression, and preprocess the data by removing 93 subjects whose gene expression is substantially different from the majority. The resulting sample size in our data analysis is then $n = 397$.

We applied our Algorithm 1 to this data set and obtained estimates of the maximal root-Pillai trace τ_{max} over a range of values of $s = s_x = s_y$. The results are displayed in Figure 5. Without adjusting for the post-selection, the sample estimate $\hat{\tau}_{\text{samp}}$ of τ_{max} increases almost linearly due to spurious correlations. On the other hand, the stabilized one-step estimator $\hat{\tau}_{\text{max}}$ gives reasonable estimates that settle down beyond $s = 15$. The confidence intervals suggest that there is a highly significant association between microRNA and gene expression (with p-value less than 10^{-10}), which is consistent with previous studies. The results for the stabilized one-step estimator are based on 10 random re-orderings of the data. The results without random re-ordering are very similar (see Figure S1 in the Supplementary Materials).

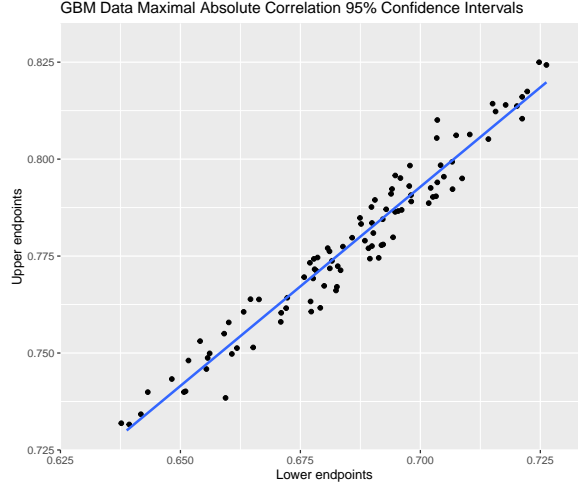


Figure 6: GBM data analysis. The lower and upper endpoints of the 95% confidence interval for τ_{\max} when $s = 1$, for 100 random re-orderings of the data.

	hsa.miR.219	hsa.miR.222	hsa.miR.138
SPIRE2	0.76	-0.27	0.50
FGF9	0.76	-0.06	0.33
ZNF553	-0.24	0.61	-0.17

Table 2: GBM data analysis. Marginal correlations between the selected genes (each row) and microRNAs (each column) at sparsity level $s = s_x = s_y = 3$. The stabilized one-step estimator $\hat{\tau}_{\max} = 0.931$ with standard error 0.085.

The random ordering of the samples has little affect on the results. For $s = s_x = s_y = 1$, we calculated the 95% confidence intervals based on 100 random re-ordering of the original data. The endpoints of the CIs are displayed in Figure 6, where each point in the scatterplot represents one CI. All the CIs have very similar widths, and are far away from zero, which is consistent with the finding of very small p-values.

Table 2 lists the most correlated variables under sparsity level $s = 3$. Interestingly, the first two microRNA measurements (*hsa.miR.219* and *hsa.miR.222*) also appear in a reported dependency network of important microRNAs obtained by precision matrix estimation (Wang, 2015, Figure 1). The top 25 microRNA and top 25 gene expressions in our analysis are provided in the Supplementary Materials.

6 Discussion

In this article, we develop a new method for sparse CCA in terms of a stabilized one-step estimator for the maximal root-Pillai trace τ_{\max} at prespecified sparsity levels. We establish the asymptotic normality of this estimator and the validity of a confidence interval for τ_{\max} when the number of variables diverge with the sample size. Based on a greedy search algorithm, we are able to obtain a computationally tractable approximate solution that is feasible even when the pre-specified sparsity levels are moderately large. Although addressing a non-regular estimation problem, the proposed stabilized one-step estimator for the targeted maximal root-Pillai trace is asymptotically efficient when it has a unique maximizing set of indices. Further, the asymptotic theory we develop also applies to the result of the greedy search algorithm (which targets a parameter that is in general close to, but not identical to, the maximal root-Pillai trace). Our simulation studies show the method performs well provided the true sparsity levels are in the range 1–10, and it outperforms Bonferroni-corrected and higher criticism MANOVA F-tests. Difficulties occur for the proposed method with weak dense signals (many small canonical correlation coefficients) due to instability in the sample coherence matrix as the prespecified sparsity levels become relatively large (≥ 20 say).

A direction for future research is the extension from linear to non-linear relationships in the setting of model-free sufficient dimension reduction (Li, 2018). Such an extension is related to the testing of predictor contributions (Cook, 2004) and the recent post-dimension reduction inference framework of Kim et al. (2020). For example, the targeted covariance matrix in sliced inverse regression (Li, 1991), namely $\text{cov}\{E(\mathbf{X} \mid \mathbf{Y})\}$, could be used in a similar role as $\Lambda_{\mathbf{X}\mathbf{Y}}$ in our setting. Methods of post-selection inference have yet to be developed in these settings as far as we know.

Acknowledgments

The authors thank Dr. Aaron Molstad from the University of Florida for sharing the pre-processed Glioblastoma Multiforme data set. IWM was supported by NIH under award 1R01 AG062401. XZ was supported by NSF under award CCF-1908969.

Appendix

A.1 Derivation of the canonical gradient

In the following derivation, we write

$$\Phi(P) = \Phi^d(P) = \|\Lambda_{\mathbf{X}\kappa\mathbf{Y}\mathcal{J}}\|_F^2 = \|\Lambda_{\mathbf{X}\mathbf{Y}}\|_F^2 = \text{tr}(\Lambda_{\mathbf{X}\mathbf{Y}}\Lambda_{\mathbf{X}\mathbf{Y}}^T) = \text{tr}(\Sigma_{\mathbf{X}}^{-1}\Sigma_{\mathbf{X}\mathbf{Y}}\Sigma_{\mathbf{Y}}^{-1}\Sigma_{\mathbf{X}\mathbf{Y}}^T).$$

Using standard results from matrix calculus,

$$\begin{aligned} d\Phi(P) &= d\text{tr}(\Sigma_{\mathbf{X}}^{-1}\Sigma_{\mathbf{X}\mathbf{Y}}\Sigma_{\mathbf{Y}}^{-1}\Sigma_{\mathbf{X}\mathbf{Y}}^T) \\ &= \frac{\partial\text{tr}(\Sigma_{\mathbf{X}}^{-1}\Sigma_{\mathbf{X}\mathbf{Y}}\Sigma_{\mathbf{Y}}^{-1}\Sigma_{\mathbf{X}\mathbf{Y}}^T)}{\partial\Sigma_{\mathbf{X}}} \cdot d\Sigma_{\mathbf{X}} + \frac{\partial\text{tr}(\Sigma_{\mathbf{X}}^{-1}\Sigma_{\mathbf{X}\mathbf{Y}}\Sigma_{\mathbf{Y}}^{-1}\Sigma_{\mathbf{X}\mathbf{Y}}^T)}{\partial\Sigma_{\mathbf{Y}}} \cdot d\Sigma_{\mathbf{Y}} \\ &\quad + \frac{\partial\text{tr}(\Sigma_{\mathbf{X}}^{-1}\Sigma_{\mathbf{X}\mathbf{Y}}\Sigma_{\mathbf{Y}}^{-1}\Sigma_{\mathbf{X}\mathbf{Y}}^T)}{\partial\Sigma_{\mathbf{X}\mathbf{Y}}} \cdot d\Sigma_{\mathbf{X}\mathbf{Y}} \\ &= -\Sigma_{\mathbf{X}}^{-1}\Sigma_{\mathbf{X}\mathbf{Y}}\Sigma_{\mathbf{Y}}^{-1}\Sigma_{\mathbf{X}\mathbf{Y}}^T\Sigma_{\mathbf{X}}^{-1} \cdot d\Sigma_{\mathbf{X}} - \Sigma_{\mathbf{Y}}^{-1}\Sigma_{\mathbf{X}\mathbf{Y}}^T\Sigma_{\mathbf{X}}^{-1}\Sigma_{\mathbf{X}\mathbf{Y}}\Sigma_{\mathbf{Y}}^{-1} \cdot d\Sigma_{\mathbf{Y}} \\ &\quad + 2\Sigma_{\mathbf{X}}^{-1}\Sigma_{\mathbf{X}\mathbf{Y}}\Sigma_{\mathbf{Y}}^{-1} \cdot d\Sigma_{\mathbf{X}\mathbf{Y}}, \end{aligned}$$

where the dot indicates inner product of two matrices of same dimension: $\mathbf{A} \cdot d\mathbf{B} = \langle \mathbf{A}, d\mathbf{B} \rangle = \text{vec}^T(\mathbf{A})\text{vec}(d\mathbf{B}) = \text{tr}(\mathbf{A}^T d\mathbf{B})$. Hence

$$\begin{aligned} \frac{d\Phi(P_\epsilon)}{d\epsilon} &= -\text{tr} \left\{ \Sigma_{\mathbf{X}}^{-1}\Sigma_{\mathbf{X}\mathbf{Y}}\Sigma_{\mathbf{Y}}^{-1}\Sigma_{\mathbf{X}\mathbf{Y}}^T\Sigma_{\mathbf{X}}^{-1} \frac{d\Sigma_{\mathbf{X}}(P_\epsilon)}{d\epsilon} \right\} \\ &\quad -\text{tr} \left\{ \Sigma_{\mathbf{Y}}^{-1}\Sigma_{\mathbf{X}\mathbf{Y}}^T\Sigma_{\mathbf{X}}^{-1}\Sigma_{\mathbf{X}\mathbf{Y}}\Sigma_{\mathbf{Y}}^{-1} \frac{d\Sigma_{\mathbf{Y}}(P_\epsilon)}{d\epsilon} \right\} + 2\text{tr} \left\{ \Sigma_{\mathbf{X}}^{-1}\Sigma_{\mathbf{X}\mathbf{Y}}\Sigma_{\mathbf{Y}}^{-1} \frac{d\Sigma_{\mathbf{X}\mathbf{Y}}(P_\epsilon)}{d\epsilon} \right\}, \end{aligned}$$

recalling that $P_\epsilon = (1 - \epsilon)P + \epsilon\delta_{\mathbf{o}}$, where $\delta_{\mathbf{o}}$ is the Dirac measure at $\mathbf{o} = (\mathbf{x}^T, \mathbf{y}^T)^T$. Expressing $\Sigma_{\mathbf{X}}(P_\epsilon)$ as

$$(1 - \epsilon)P(\mathbf{X}\mathbf{X}^T) + \epsilon\mathbf{x}\mathbf{x}^T - (1 - \epsilon)^2P(\mathbf{X})P(\mathbf{X}^T) - \epsilon(1 - \epsilon)\{P(\mathbf{X})\mathbf{x}^T + \mathbf{x}P(\mathbf{X}^T)\} - \epsilon^2\mathbf{x}\mathbf{x}^T,$$

by direct calculation we then have

$$\left. \frac{d\Sigma_{\mathbf{X}}(P_\epsilon)}{d\epsilon} \right|_{\epsilon=0} = \lim_{\epsilon \downarrow 0} \frac{\Sigma_{\mathbf{X}}(P_\epsilon) - \Sigma_{\mathbf{X}}(P)}{\epsilon} = \{\mathbf{x} - P(\mathbf{X})\}\{\mathbf{x}^T - P(\mathbf{X}^T)\}.$$

Similarly,

$$\left. \frac{d\Sigma_{\mathbf{X}\mathbf{Y}}(P_\epsilon)}{d\epsilon} \right|_{\epsilon=0} = \{\mathbf{x} - P(\mathbf{X})\}\{\mathbf{y}^T - P(\mathbf{Y}^T)\}, \quad \left. \frac{d\Sigma_{\mathbf{Y}}(P_\epsilon)}{d\epsilon} \right|_{\epsilon=0} = \{\mathbf{y} - P(\mathbf{Y})\}\{\mathbf{y}^T - P(\mathbf{Y}^T)\}.$$

Plugging-in these expressions, and including the relevant sets of indices \mathcal{K} and \mathcal{J} , we obtain canonical gradient of $\Phi^d(P)$ as stated in (5):

$$\begin{aligned} \left. \frac{d\Phi^d(P_\epsilon)}{d\epsilon} \right|_{\epsilon=0} &= -\{\mathbf{x}_{\mathcal{K}} - \mathbb{E}_P(\mathbf{X}_{\mathcal{K}})\}^T \Sigma_{\mathbf{X}_{\mathcal{K}}}^{-1} \Sigma_{\mathbf{X}_{\mathcal{K}}\mathbf{Y}_{\mathcal{J}}} \Sigma_{\mathbf{Y}_{\mathcal{J}}}^{-1} \Sigma_{\mathbf{Y}_{\mathcal{J}}\mathbf{X}_{\mathcal{K}}} \Sigma_{\mathbf{X}_{\mathcal{K}}}^{-1} \{\mathbf{x}_{\mathcal{K}} - \mathbb{E}_P(\mathbf{X}_{\mathcal{K}})\} \\ &\quad -\{\mathbf{y}_{\mathcal{J}} - \mathbb{E}_P(\mathbf{Y}_{\mathcal{J}})\}^T \Sigma_{\mathbf{Y}_{\mathcal{J}}}^{-1} \Sigma_{\mathbf{Y}_{\mathcal{J}}\mathbf{X}_{\mathcal{K}}} \Sigma_{\mathbf{X}_{\mathcal{K}}}^{-1} \Sigma_{\mathbf{X}_{\mathcal{K}}\mathbf{Y}_{\mathcal{J}}} \Sigma_{\mathbf{Y}_{\mathcal{J}}}^{-1} \{\mathbf{y}_{\mathcal{J}} - \mathbb{E}_P(\mathbf{Y}_{\mathcal{J}})\} \\ &\quad +2\{\mathbf{y}_{\mathcal{J}} - \mathbb{E}_P(\mathbf{Y}_{\mathcal{J}})\}^T \Sigma_{\mathbf{Y}_{\mathcal{J}}}^{-1} \Sigma_{\mathbf{Y}_{\mathcal{J}}\mathbf{X}_{\mathcal{K}}} \Sigma_{\mathbf{X}_{\mathcal{K}}}^{-1} \{\mathbf{x}_{\mathcal{K}} - \mathbb{E}_P(\mathbf{X}_{\mathcal{K}})\}. \end{aligned}$$

Then, as discussed in Section 2.2, the canonical gradient of $\Psi^d(P) = \|\Lambda_{\mathbf{X}_{\mathcal{K}}\mathbf{Y}_{\mathcal{J}}}\|_F$ is obtained via the relationship $\{\Psi^d(P)\}^2 = \Phi^d(P)$, resulting in

$$D^d(P)(\mathbf{O}) = \left. \frac{d\Psi^d(P_\epsilon)}{d\epsilon} \right|_{\epsilon=0} = \frac{1}{2\Psi^d(P)} \left. \frac{d\Phi^d(P_\epsilon)}{d\epsilon} \right|_{\epsilon=0}$$

when $\Psi^d(P) \neq 0$.

To prove $\mathbb{E}_P\{D^d(P)(\mathbf{O})\} = 0$ it suffices to show that the canonical gradient of $\Phi^d(P)$ has zero mean. We apply the following property of trace and expectation operators. For any random vector $\mathbf{X} \in \mathbb{R}^p$ with entries having finite second moments and any non-stochastic matrix $\mathbf{M} \in \mathbb{R}^{p \times p}$,

$$\mathbb{E}(\mathbf{X}^T \mathbf{M} \mathbf{X}) = \mathbb{E}\{\text{tr}(\mathbf{X}^T \mathbf{M} \mathbf{X})\} = \mathbb{E}\{\text{tr}(\mathbf{M} \mathbf{X} \mathbf{X}^T)\} = \text{tr}\{\mathbf{M} \mathbb{E}(\mathbf{X} \mathbf{X}^T)\}. \quad (\text{A.1})$$

Therefore, direct calculation shows that

$$\begin{aligned} \mathbb{E} \left\{ \left. \frac{d\Phi^d(P_\epsilon)}{d\epsilon} \right|_{\epsilon=0} \right\} &= -\text{tr} \left(\Sigma_{\mathbf{X}_{\mathcal{K}}}^{-1} \Sigma_{\mathbf{X}_{\mathcal{K}}\mathbf{Y}_{\mathcal{J}}} \Sigma_{\mathbf{Y}_{\mathcal{J}}}^{-1} \Sigma_{\mathbf{Y}_{\mathcal{J}}\mathbf{X}_{\mathcal{K}}} \Sigma_{\mathbf{X}_{\mathcal{K}}}^{-1} \cdot \mathbb{E}_P \left[\{\mathbf{X}_{\mathcal{K}} - \mathbb{E}_P(\mathbf{X}_{\mathcal{K}})\} \{\mathbf{X}_{\mathcal{K}} - \mathbb{E}_P(\mathbf{X}_{\mathcal{K}})\}^T \right] \right) \\ &\quad -\text{tr} \left(\Sigma_{\mathbf{Y}_{\mathcal{J}}}^{-1} \Sigma_{\mathbf{Y}_{\mathcal{J}}\mathbf{X}_{\mathcal{K}}} \Sigma_{\mathbf{X}_{\mathcal{K}}}^{-1} \Sigma_{\mathbf{X}_{\mathcal{K}}\mathbf{Y}_{\mathcal{J}}} \Sigma_{\mathbf{Y}_{\mathcal{J}}}^{-1} \cdot \mathbb{E}_P \left[\{\mathbf{Y}_{\mathcal{J}} - \mathbb{E}_P(\mathbf{Y}_{\mathcal{J}})\} \{\mathbf{Y}_{\mathcal{J}} - \mathbb{E}_P(\mathbf{Y}_{\mathcal{J}})\}^T \right] \right) \\ &\quad +2\text{tr} \left(\Sigma_{\mathbf{Y}_{\mathcal{J}}}^{-1} \Sigma_{\mathbf{Y}_{\mathcal{J}}\mathbf{X}_{\mathcal{K}}} \Sigma_{\mathbf{X}_{\mathcal{K}}}^{-1} \cdot \mathbb{E}_P \left[\{\mathbf{X}_{\mathcal{K}} - \mathbb{E}_P(\mathbf{X}_{\mathcal{K}})\} \{\mathbf{Y}_{\mathcal{J}} - \mathbb{E}_P(\mathbf{Y}_{\mathcal{J}})\}^T \right] \right) \\ &= -\Phi^d(P) - \Phi^d(P) + 2\Phi^d(P) = 0. \end{aligned}$$

When $\Psi^d(P) = 0$, using instead the expression (6) for the canonical gradient and again applying (A.1) we obtain

$$\begin{aligned} \mathbb{E}_P\{D^d(P)(\mathbf{O})\} &= \mathbb{E}_P \left[\{\mathbf{Y}_{\mathcal{J}} - \mathbb{E}_P(\mathbf{Y}_{\mathcal{J}})\}^T \Sigma_{\mathbf{Y}_{\mathcal{J}}}^{-1/2} \mathbf{L} \Sigma_{\mathbf{X}_{\mathcal{K}}}^{-1/2} \{\mathbf{X}_{\mathcal{K}} - \mathbb{E}_P(\mathbf{X}_{\mathcal{K}})\} \right] \\ &= \text{tr} \left(\mathbf{L} \Sigma_{\mathbf{X}_{\mathcal{K}}}^{-1/2} \mathbb{E}_P \left[\{\mathbf{X}_{\mathcal{K}} - \mathbb{E}_P(\mathbf{X}_{\mathcal{K}})\} \{\mathbf{Y}_{\mathcal{J}} - \mathbb{E}_P(\mathbf{Y}_{\mathcal{J}})\}^T \right] \Sigma_{\mathbf{Y}_{\mathcal{J}}}^{-1/2} \right) \\ &= \text{tr}(\mathbf{L} \Lambda_{\mathbf{X}_{\mathcal{K}}\mathbf{Y}_{\mathcal{J}}}) = 0 \end{aligned}$$

since $\Lambda_{\mathbf{X}_{\mathcal{K}}\mathbf{Y}_{\mathcal{J}}} = 0$ when $\Psi^d(P) = 0$.

A.2 Proof of Lemma 1

Let $\mathbb{X} \in \mathbb{R}^{n \times s_x}$, $\mathbb{Y} \in \mathbb{R}^{n \times s_y}$ and $\mathbb{Z} \in \mathbb{R}^{n \times 1}$ be the centered data matrices of $\mathbf{X}_{\mathcal{K}}$, $\mathbf{Y}_{\mathcal{J}}$ and X_k . That is, the i -th row of \mathbb{X} is $(\mathbf{X}_{\mathcal{K},i} - \bar{\mathbf{X}}_{\mathcal{K}})^T$. Note that $\mathbf{S}_{\mathbf{X}_{\mathcal{K}}} = \mathbb{X}\mathbb{X}^T/n$ is the sample covariance matrix of $\mathbf{X}_{\mathcal{K}}$, which is assumed to be positive definite. Then we can write $\mathbf{C}_{\mathbf{Y}_{\mathcal{J}}\mathbf{X}_{\mathcal{K}}} = n^{-1}\mathbf{S}_{\mathbf{Y}_{\mathcal{J}}}^{-1/2}\mathbb{Y}^T\mathbb{X}\mathbf{S}_{\mathbf{X}_{\mathcal{K}}}^{-1/2}$ and $\mathbf{C}_{\mathbf{Y}_{\mathcal{J}}\mathbf{X}_{\mathcal{K}}}\mathbf{C}_{\mathbf{Y}_{\mathcal{J}}\mathbf{X}_{\mathcal{K}}}^T = n^{-1}\mathbf{S}_{\mathbf{Y}_{\mathcal{J}}}^{-1/2}\mathbb{Y}^T\mathbb{X}(\mathbb{X}^T\mathbb{X})^{-1}\mathbb{X}^T\mathbb{Y}\mathbf{S}_{\mathbf{Y}_{\mathcal{J}}}^{-1/2}$, where $\mathbb{X}(\mathbb{X}^T\mathbb{X})^{-1}\mathbb{X}^T \equiv \mathbf{P}_{\mathbb{X}} \in \mathbb{R}^{n \times n}$ is the projection matrix onto the s_x -dimensional subspace spanned by the columns of \mathbb{X} . Then,

$$\|\mathbf{C}_{\mathbf{Y}_{\mathcal{J}}\mathbf{X}_{\mathcal{K}}}\|_F^2 = \text{tr}(\mathbf{C}_{\mathbf{Y}_{\mathcal{J}}\mathbf{X}_{\mathcal{K}}}\mathbf{C}_{\mathbf{Y}_{\mathcal{J}}\mathbf{X}_{\mathcal{K}}}^T) = n^{-1}\text{tr}(\mathbf{S}_{\mathbf{Y}_{\mathcal{J}}}^{-1/2}\mathbb{Y}^T\mathbf{P}_{\mathbb{X}}\mathbb{Y}\mathbf{S}_{\mathbf{Y}_{\mathcal{J}}}^{-1/2}), \quad (\text{A.2})$$

$$\|\mathbf{C}_{\mathbf{Y}_{\mathcal{J}}\mathbf{X}_{\mathcal{K} \cup \mathcal{K}_k}}\|_F^2 - \|\mathbf{C}_{\mathbf{Y}_{\mathcal{J}}\mathbf{X}_{\mathcal{K}}}\|_F^2 = n^{-1}\text{tr}\{\mathbf{S}_{\mathbf{Y}_{\mathcal{J}}}^{-1/2}\mathbb{Y}^T(\mathbf{P}_{(\mathbb{X},\mathbb{Z})} - \mathbf{P}_{\mathbb{X}})\mathbb{Y}\mathbf{S}_{\mathbf{Y}_{\mathcal{J}}}^{-1/2}\}, \quad (\text{A.3})$$

where $\mathbf{P}_{(\mathbb{X},\mathbb{Z})} \in \mathbb{R}^{n \times n}$ is the projection matrix onto the (s_x+1) -dimensional subspace of \mathbb{R}^n spanned by the columns of (\mathbb{X}, \mathbb{Z}) . That is,

$$\begin{aligned} \mathbf{P}_{(\mathbb{X},\mathbb{Z})} &= (\mathbb{X} \ \mathbb{Z}) \begin{pmatrix} \mathbb{X}^T\mathbb{X} & \mathbb{X}^T\mathbb{Z} \\ \mathbb{Z}^T\mathbb{X} & \mathbb{Z}^T\mathbb{Z} \end{pmatrix}^{-1} \begin{pmatrix} \mathbb{X}^T \\ \mathbb{Z}^T \end{pmatrix} \\ &= n^{-1} (\mathbb{X} \ \mathbb{Z}) \begin{pmatrix} \mathbf{S}_{\mathbf{X}_{\mathcal{K}}}^{-1} + \mathbf{S}_{\mathbf{X}_{\mathcal{K}}}^{-1}\mathbf{S}_{\mathbf{X}_{\mathcal{K}}X_k}\mathbf{S}_{R_k}^{-1}\mathbf{S}_{X_kX_{\mathcal{K}}}\mathbf{S}_{\mathbf{X}_{\mathcal{K}}}^{-1} & -\mathbf{S}_{\mathbf{X}_{\mathcal{K}}}^{-1}\mathbf{S}_{\mathbf{X}_{\mathcal{K}}X_k}\mathbf{S}_{R_k}^{-1} \\ -\mathbf{S}_{R_k}^{-1}\mathbf{S}_{X_kX_{\mathcal{K}}}\mathbf{S}_{\mathbf{X}_{\mathcal{K}}}^{-1} & \mathbf{S}_{R_k}^{-1} \end{pmatrix} \begin{pmatrix} \mathbb{X}^T \\ \mathbb{Z}^T \end{pmatrix} \\ &= n^{-1}\mathbb{X}\mathbf{S}_{\mathbf{X}_{\mathcal{K}}}^{-1}\mathbb{X}^T + n^{-1}(\mathbb{Z} - \mathbb{X}\mathbf{S}_{\mathbf{X}_{\mathcal{K}}}^{-1}\mathbf{S}_{\mathbf{X}_{\mathcal{K}}X_k})\mathbf{S}_{R_k}^{-1}(\mathbb{Z}^T - \mathbf{S}_{X_kX_{\mathcal{K}}}\mathbf{S}_{\mathbf{X}_{\mathcal{K}}}^{-1}\mathbb{X}^T), \\ &= \mathbf{P}_{\mathbb{X}} + \mathbf{P}_{\mathbb{Z}|\mathbb{X}}, \end{aligned}$$

where $\mathbf{S}_{R_k} = n^{-1}\{\mathbb{Z}^T\mathbb{Z} - \mathbb{Z}^T\mathbb{X}(\mathbb{X}^T\mathbb{X})^{-1}\mathbb{X}^T\mathbb{Z}\}$ is the sample covariance of the fitted residual $(\mathbb{Z} - \mathbb{X}\mathbf{S}_{\mathbf{X}_{\mathcal{K}}}^{-1}\mathbf{S}_{\mathbf{X}_{\mathcal{K}}X_k})$. Specifically, $(\mathbb{Z} - \mathbb{X}\mathbf{S}_{\mathbf{X}_{\mathcal{K}}}^{-1}\mathbf{S}_{\mathbf{X}_{\mathcal{K}}X_k})^T(\mathbb{Z} - \mathbb{X}\mathbf{S}_{\mathbf{X}_{\mathcal{K}}}^{-1}\mathbf{S}_{\mathbf{X}_{\mathcal{K}}X_k}) = n\mathbf{S}_{R_k}$. Therefore, $\mathbf{P}_{\mathbb{Z}|\mathbb{X}} \in \mathbb{R}^{n \times n}$ is indeed the projection matrix onto the one-dimensional subspace spanned by $(\mathbb{Z} - \mathbb{X}\mathbf{S}_{\mathbf{X}_{\mathcal{K}}}^{-1}\mathbf{S}_{\mathbf{X}_{\mathcal{K}}X_k})$. The conclusion follows from (A.2), (A.3) and $\mathbf{P}_{(\mathbb{X},\mathbb{Z})} = \mathbf{P}_{\mathbb{X}} + \mathbf{P}_{\mathbb{Z}|\mathbb{X}}$.

A.3 Recursive computation of the one-step estimator

In the implementation, given a new observation \mathbf{O}_{j+1} , we need to update the weight $w_j = \bar{\sigma}_n/\hat{\sigma}_j$ and the variance of the canonical gradient $\hat{\sigma}_j^2$ in order to update the current estimate ψ_j of the target parameter τ_{\max} . Since we only need to know these quantities when all observations are included, an efficient approach is to exploit the following recursive properties of $\psi_j/\bar{\sigma}_j$ and $\bar{\sigma}_j^{-1}$:

$$\frac{\psi_{j+1}}{\bar{\sigma}_{j+1}} = \frac{1}{j+1} \left\{ j \cdot \frac{\psi_j}{\bar{\sigma}_j} + \frac{\Psi^{d_{nj}}(P_j) + D^{d_j}(P_j)(\mathbf{O}_{j+1})}{\hat{\sigma}_{nj}} \right\}, \quad \bar{\sigma}_{j+1}^{-1} = \frac{1}{j+1} (j \cdot \bar{\sigma}_j^{-1} + \hat{\sigma}_{nj}^{-1}).$$

We then obtain the final estimate when $j = n$:

$$\hat{\tau}_{\max} \equiv \psi_n = \frac{\bar{\sigma}_n}{n - \ell_n} \sum_{j=\ell_n}^{n-1} \left\{ \frac{\Psi^{d_{nj}}(P_j) + D^{d_j}(P_j)(\mathbf{O}_{j+1})}{\hat{\sigma}_{nj}} \right\}, \quad \bar{\sigma}_n^{-1} = \frac{1}{n - \ell_n} \sum_{j=\ell_n}^{n-1} \hat{\sigma}_{nj}^{-1}.$$

References

- Andrews, D. (2000). Inconsistency of the bootstrap when a parameter is on the boundary of the parameter space. *Econometrica*, 68:399–405.
- Bao, Z., Hu, J., Pan, G., and Zhou, W. (2019). Canonical correlation coefficients of high-dimensional Gaussian vectors: Finite rank case. *The Annals of Statistics*, 47(1):612–640.
- Cook, R. D. (2004). Testing predictor contributions in sufficient dimension reduction. *The Annals of Statistics*, 32(3):1062–1092.
- Davies, R. B. (1977). Hypothesis testing when a nuisance parameter is present only under the alternative. *Biometrika*, 64(2):247–254.
- Davies, R. B. (1987). Hypothesis testing when a nuisance parameter is present only under the alternative. *Biometrika*, 74(1):33–43.
- Davies, R. B. (2002). Hypothesis testing when a nuisance parameter is present only under the alternative: linear model case. *Biometrika*, 89:484–489.
- Devlin, S. J., Gnanadesikan, R., and Kettenring, J. R. (1975). Robust estimation and outlier detection with correlation coefficients. *Biometrika*, 62(3):531–545.
- Donoho, D. and Jin, J. (2004). Higher criticism for detecting sparse heterogeneous mixtures. *The Annals of Statistics*, 32(3):962–994.
- Donoho, D. and Jin, J. (2015). Higher criticism for large-scale inference, especially for rare and weak effects. *Statistical Science*, 30:1–25.
- Gao, C., Ma, Z., and Zhou, H. H. (2017). Sparse CCA: Adaptive estimation and computational barriers. *The Annals of Statistics*, 45(5):2074–2101.
- Hansen, B. E. (1996). Inference when a nuisance parameter is not identified under the null hypothesis. *Econometrica: Journal of the Econometric Society*, 64:413–430.
- Hardoon, D. R. and Shawe-Taylor, J. (2011). Sparse canonical correlation analysis. *Machine Learning*, 83(3):331–353.
- Hotelling, H. (1936). Relations between two sets of variates. *Biometrika*, 28(3-4):321–377.
- Khim, J. T., Jog, V., and Loh, P.-L. (2016). Computing and maximizing influence in linear threshold and triggering models. In *Advances in Neural Information Processing Systems*, pages 4538–4546.

- Kim, K., Li, B., Yu, Z., and Li, L. (2020). On post dimension reduction statistical inference. *The Annals of Statistics*, 48(3):1567–1592.
- Krause, A. and Golovin, D. (2014). Submodular function maximization. In *Tractability: Practical Approaches to Hard Problems*. Cambridge University Press.
- Leeb, H. and Pötscher, B. M. (2017). Testing in the presence of nuisance parameters: Some comments on tests post-model-selection and random critical values. In *Big and Complex Data Analysis: Methodologies and Applications*, pages 69–82. Springer International Publishing.
- Li, B. (2018). *Sufficient Dimension Reduction: Methods and Applications with R*. CRC Press.
- Li, K.-C. (1991). Sliced inverse regression for dimension reduction. *Journal of the American Statistical Association*, 86(414):316–327.
- Luedtke, A. R. and van der Laan, M. (2018). Parametric-rate inference for one-sided differentiable parameters. *Journal of the American Statistical Association*, 113(522):780–788.
- Mai, Q. and Zhang, X. (2019). An iterative penalized least squares approach to sparse canonical correlation analysis. *Biometrics*, 75(3):734–744.
- McKeague, I. W. and Qian, M. (2015). An adaptive resampling test for detecting the presence of significant predictors. *Journal of the American Statistical Association*, 110(512):1422–1433.
- Molstad, A. J. (2019). Insights and algorithms for the multivariate square-root lasso. *arXiv preprint arXiv:1909.05041*.
- Naylor, M. G., Lin, X., Weiss, S. T., Raby, B. A., and Lange, C. (2010). Using canonical correlation analysis to discover genetic regulatory variants. *PLOS ONE*, 5(5):1–6.
- Nemhauser, G. L. and Wolsey, L. A. (1978). Best algorithms for approximating the maximum of a submodular set function. *Mathematics of Operations Research*, 3(3):177–188.
- Parkhomenko, E., Tritchler, D., and Beyene, J. (2009). Sparse canonical correlation analysis with application to genomic data integration. *Statistical applications in genetics and molecular biology*, 8(1).
- Pfanzagl, J. (1982). Contributions to a general asymptotic statistical theory. *Lecture Notes in Statistics*, 13.
- Pfanzagl, J. (1990). *Estimation in Semiparametric Models*. Springer.
- Pillai, K. C. S. (1955). Some new test criteria in multivariate analysis. *The Annals of Mathematical Statistics*, 26:117–121.
- Qadar, M. and Seghouane, A.-K. (2019). A projection CCA method for effective fMRI data analysis. *IEEE Transactions on Biomedical Engineering*, 66(11):3247–3256.
- Seghouane, A.-K. and Shokouhi, N. (2019). Estimating the number of significant canonical coordinates. *IEEE Access*, 7:108806–108817.

- Shu, H., Wang, X., and Zhu, H. (2020). D-CCA: A decomposition-based canonical correlation analysis for high-dimensional datasets. *Journal of the American Statistical Association*, 115(529):292–306.
- Song, Y., Schreier, P. J., Ramirez, D., and Hasija, T. (2016). Canonical correlation analysis of high-dimensional data with very small sample support. *Signal Processing*, 128:449 – 458.
- Tibshirani, R. (1996). Regression shrinkage and selection via the lasso. *Journal of the Royal Statistical Society: Series B*, 58(1):267–288.
- van der Laan, M. J. and Lendle, S. D. (2014). Online Targeted Learning. Technical Report 330, Division of Biostatistics, University of California, Berkeley. Available at <http://www.bepress.com/ucbbiostat/>.
- van der Vaart, A. W. (2000). *Asymptotic Statistics*. Cambridge University Press.
- Waaijenborg, S., Verselewele de Witt Hamer, P. C., and H., Z. A. (2008). Quantifying the Association between Gene Expressions and DNA-Markers by Penalized Canonical Correlation Analysis. *Statistical Applications in Genetics and Molecular Biology*, 7(1):1–29.
- Waaijenborg, S. and Zwinderman, A. H. (2007). Penalized canonical correlation analysis to quantify the association between gene expression and DNA markers. *BMC Proceedings*, 1(1):S122.
- Wang, J. (2015). Joint estimation of sparse multivariate regression and conditional graphical models. *Statistica Sinica*, 25:831–851.
- Wang, Y. R., Jiang, K., Feldman, L. J., Bickel, P. J., Huang, H., et al. (2015). Inferring gene–gene interactions and functional modules using sparse canonical correlation analysis. *The Annals of Applied Statistics*, 9(1):300–323.
- Weinstein, J. N., Collisson, E. A., Mills, G. B., Shaw, K. R. M., Ozenberger, B. A., Ellrott, K., Shmulevich, I., Sander, C., Stuart, J. M., Network, C. G. A. R., et al. (2013). The cancer genome atlas pan-cancer analysis project. *Nature Genetics*, 45(10):1113.
- Wiesel, A., Kliger, M., and Hero, A. O. (2008). A greedy approach to sparse canonical correlation analysis. arXiv: 0801.2748.
- Witten, D. M., Tibshirani, R., and Hastie, T. (2009). A penalized matrix decomposition, with applications to sparse principal components and canonical correlation analysis. *Biostatistics*, 10(3):515–534.
- Yang, Y. and Pan, G. (2015). Independence test for high dimensional data based on regularized canonical correlation coefficients. *Ann. Statist.*, 43(2):467–500.
- Zheng, S., Cheng, G., Guo, J., and Zhu, H. (2019). Test for high-dimensional correlation matrices. *The Annals of Statistics*, 47:2887–2921.
- Zou, H. and Hastie, T. (2005). Regularization and variable selection via the elastic net. *Journal of the Royal Statistical Society: Series B*, 67(2):301–320.